74th MidWest PDE Meeting

Network Formation in Amphiphilic Polymer Materials

Oct 18-19, 2014

Keith Promislow

MICHIGAN STATE UNIVERSITY

MICHIGAN STATE UNIVERSITY

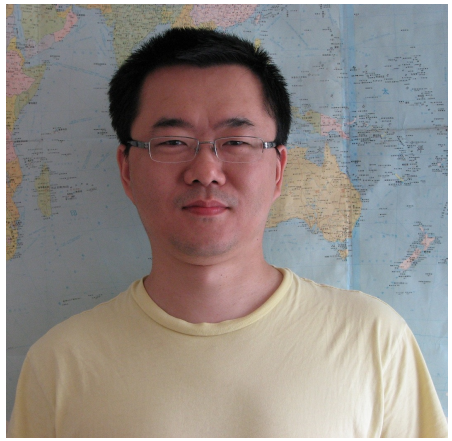

Shibin Dai

Noa Kraitzman

Andrew Christlieb

Zhengfu Xu

Qiliang Wu

Greg Hayrapetyan

Jaylan Jones

Brian Wetton

Role of Solvent in Cast-Driven Morphology

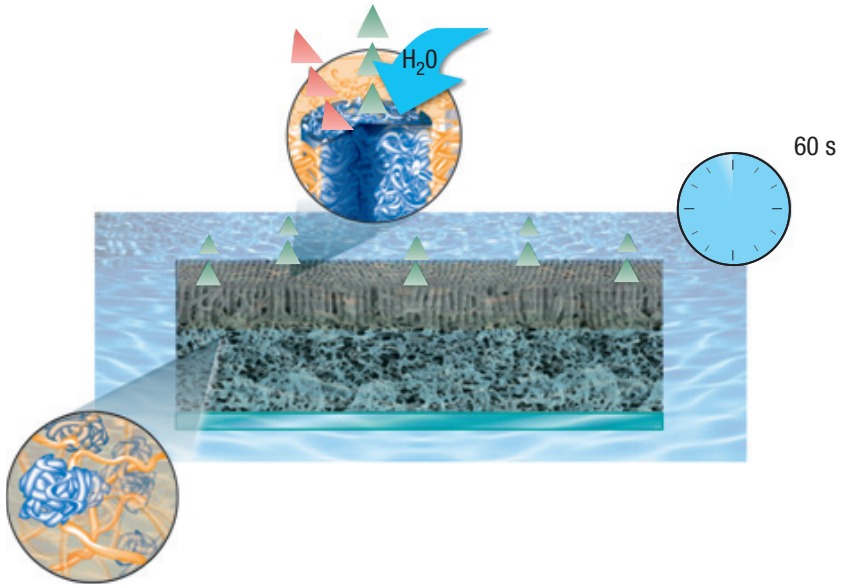

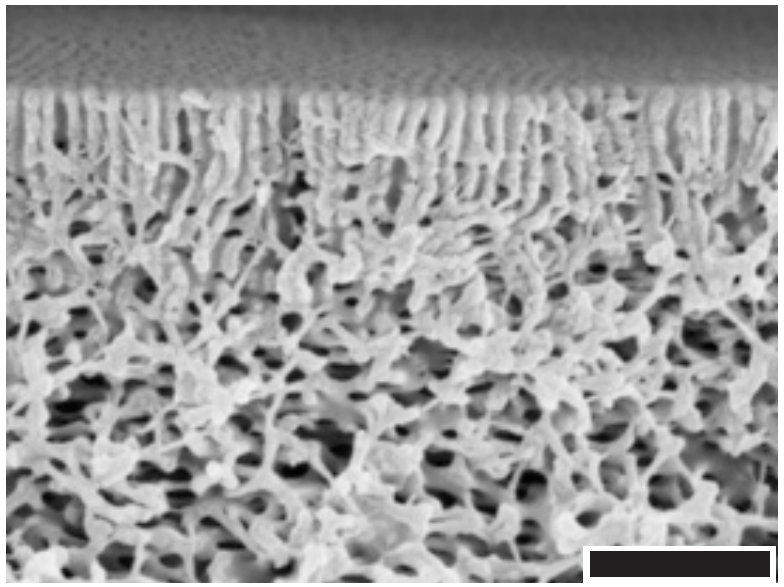

Mix two miscible solvents (DMF and THF) with an amphiphilic di-block co-polymer (PEO-poly vinyl pyridine) one of whose components is soluble only in DMF. Evaporating off the THF changes the ”goodness” of the solvent. Then immerse in water.
K.-V. Peinemann, V. Abetz, P. F. Simon, *Nature Materials* (2007)

Ionomer Membranes: Selective charge transport

NAFION

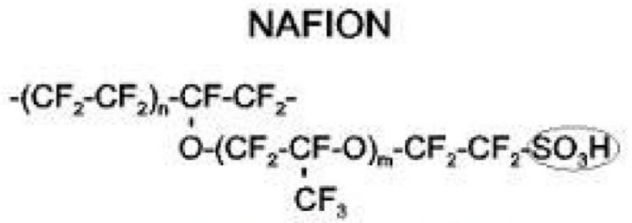

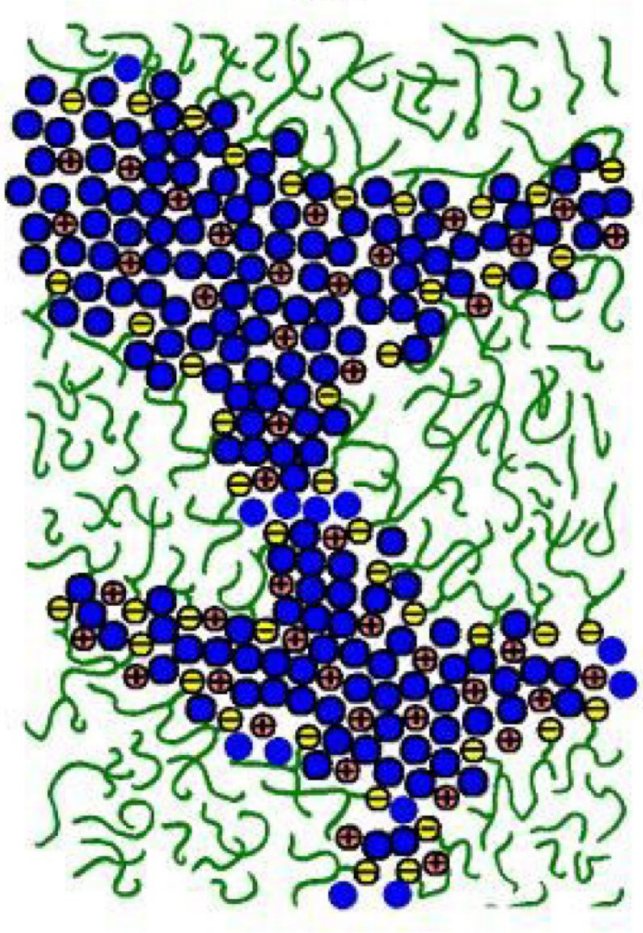

Ionomer Membranes: Incorporation of Solvation Energy

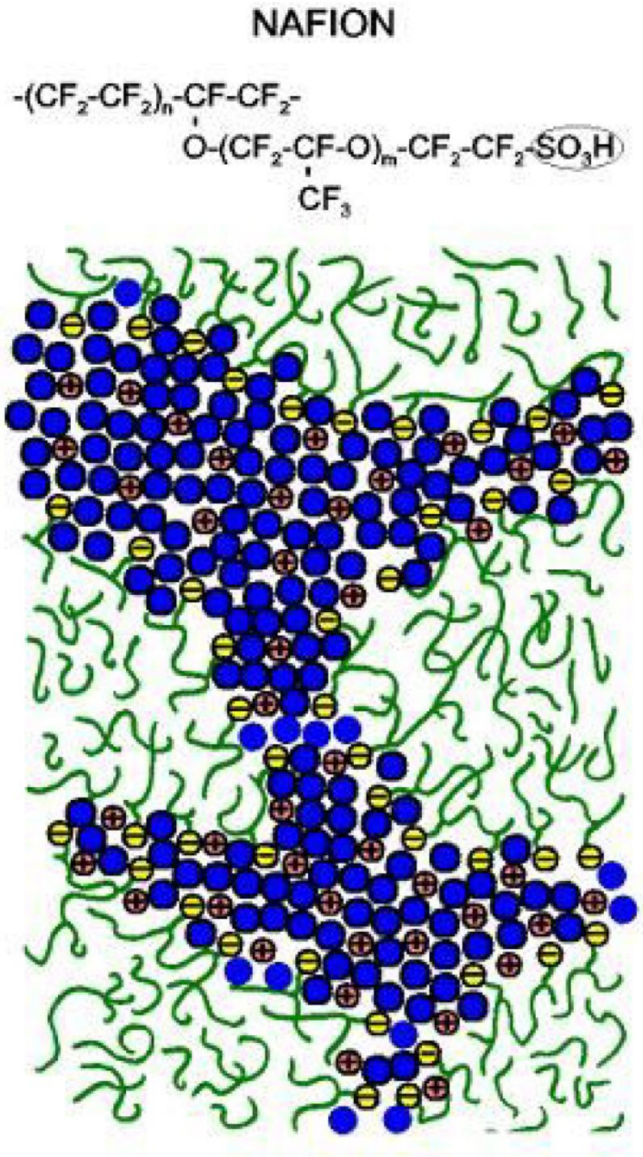

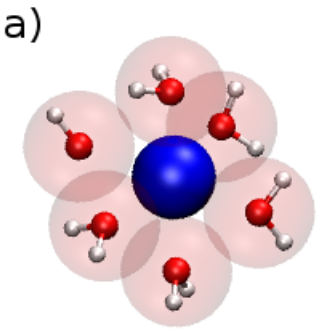

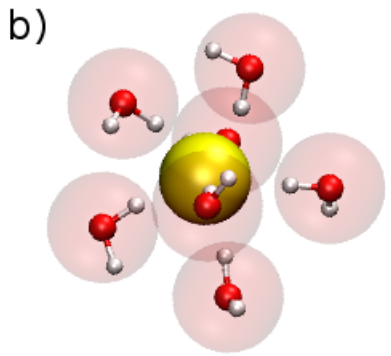

Na^+

F^-

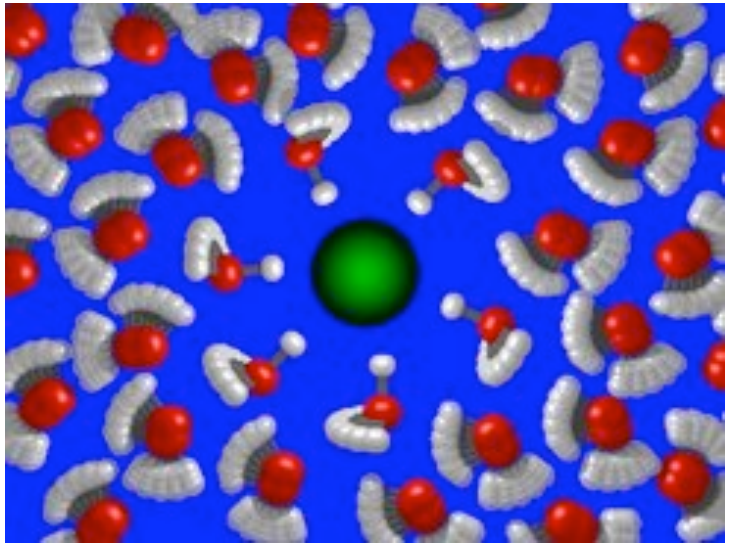

Ionomer Membranes: Incorporation of Solvation Energy

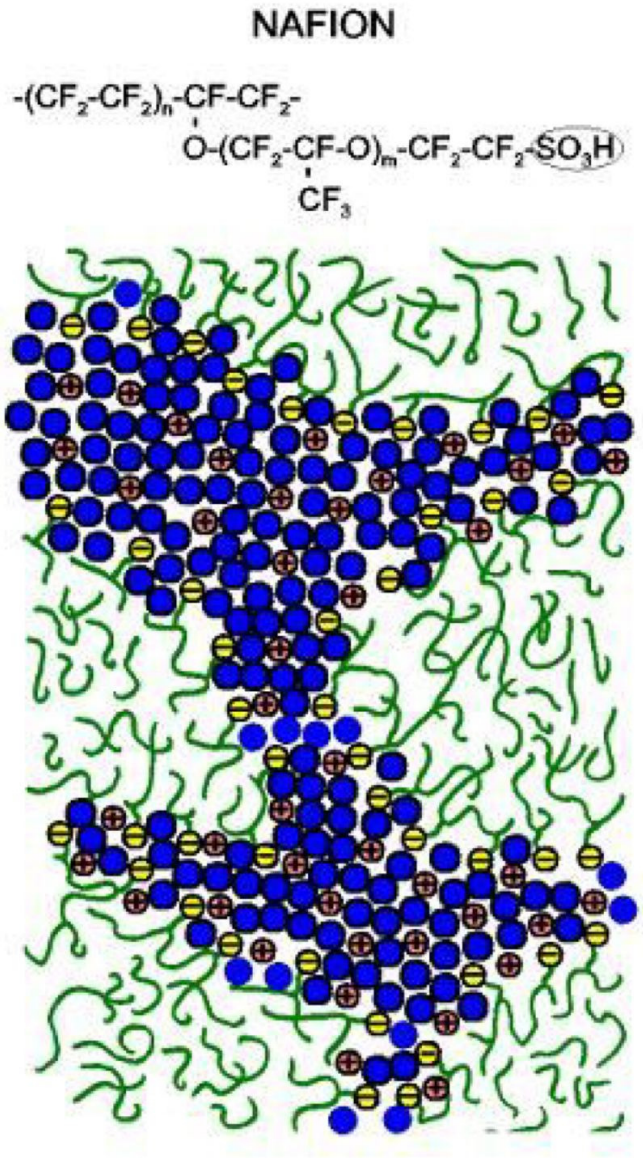

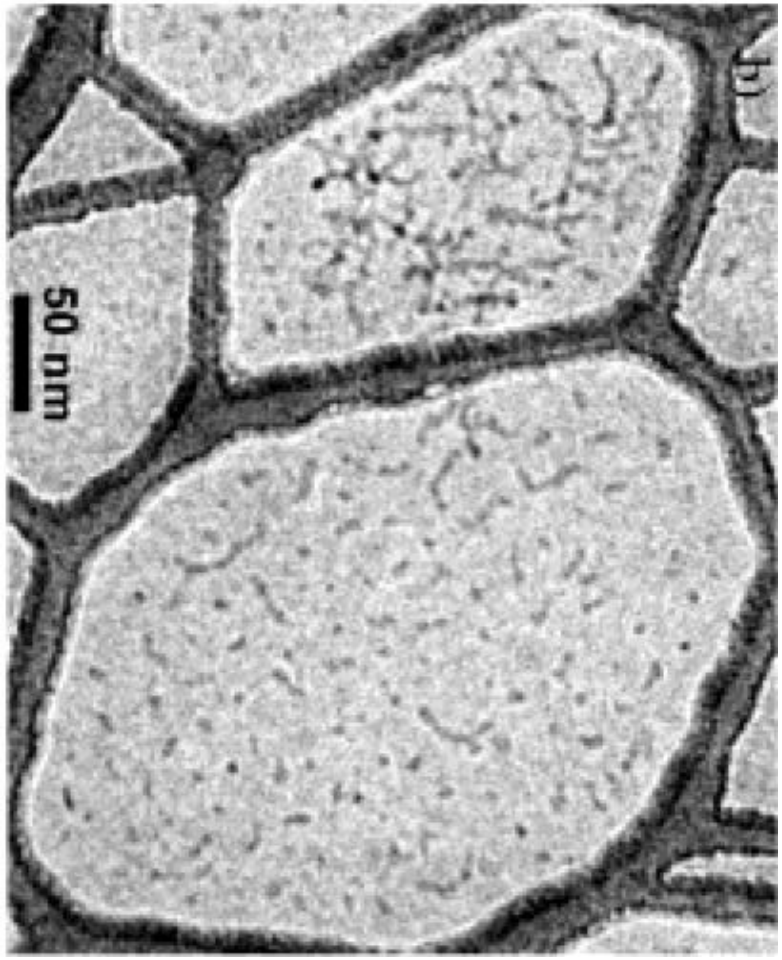

Diat 2004 *Macro.* TEM of Cs^{+}-Nafion

Ionomer Membranes: Incorporation of Solvation Energy

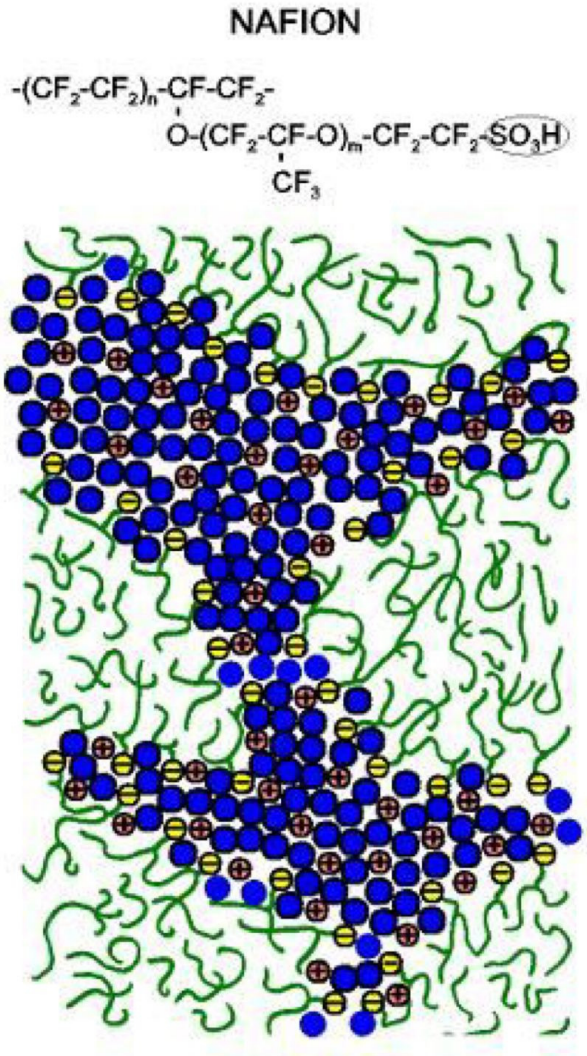

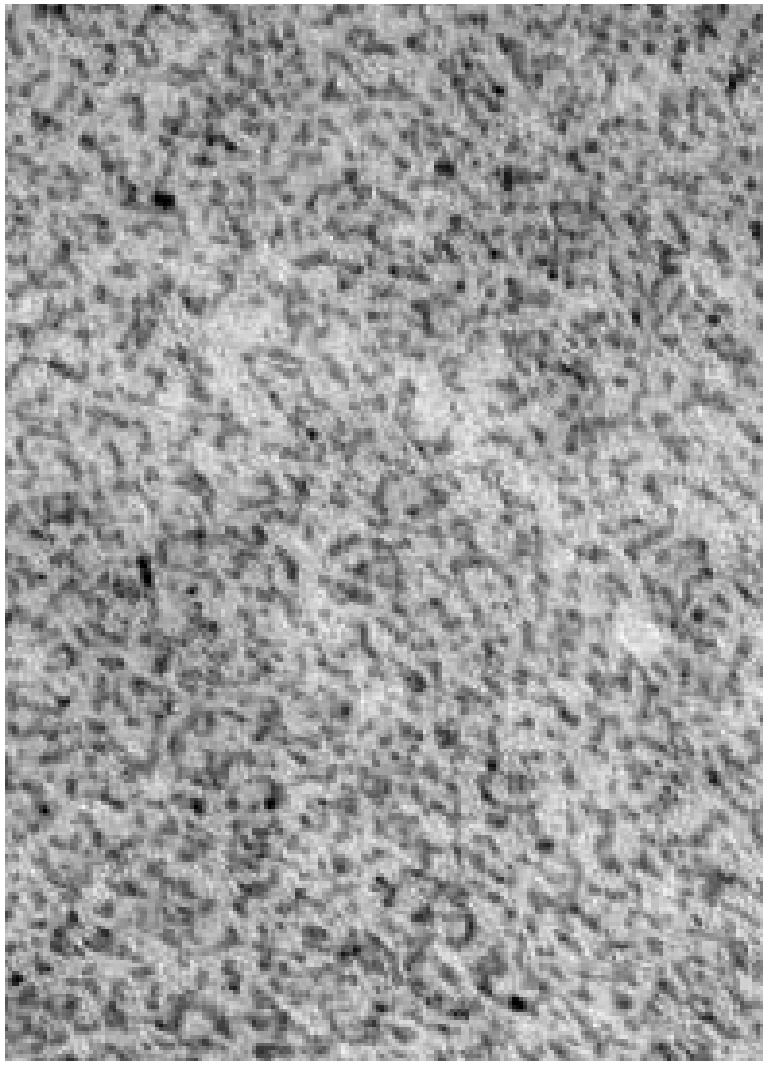

TEM of Cu^{+2}-Nafion

Salt Molarity and Solvation

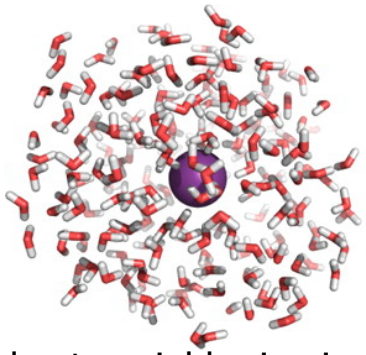

Field due to neighboring ions negligible

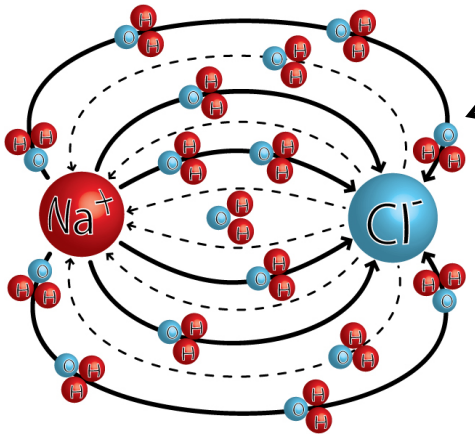

Field due to neighboring ions not negligible
Water screening important

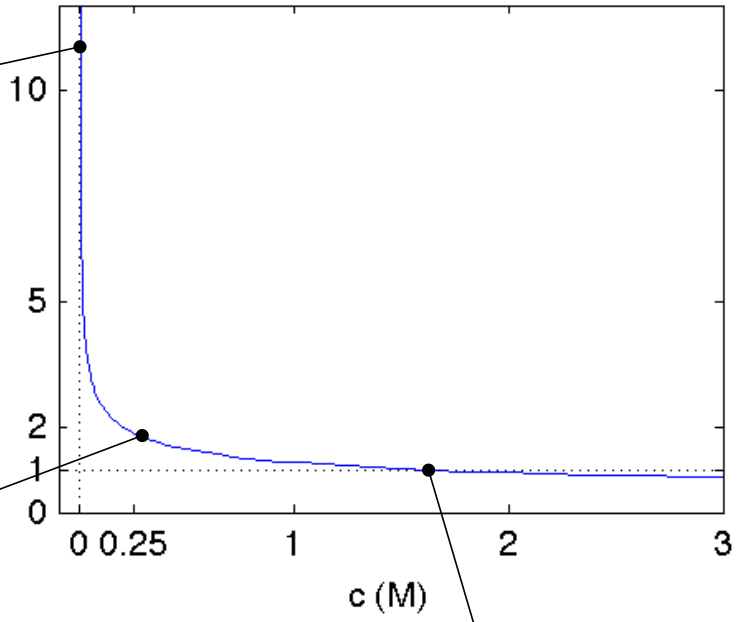

1 nm between ions
Fitting 1-2 water molecules

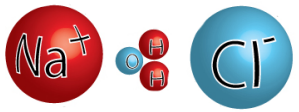

Ionic field dominant
Water screening negligible

Ion Size and Ion Packing

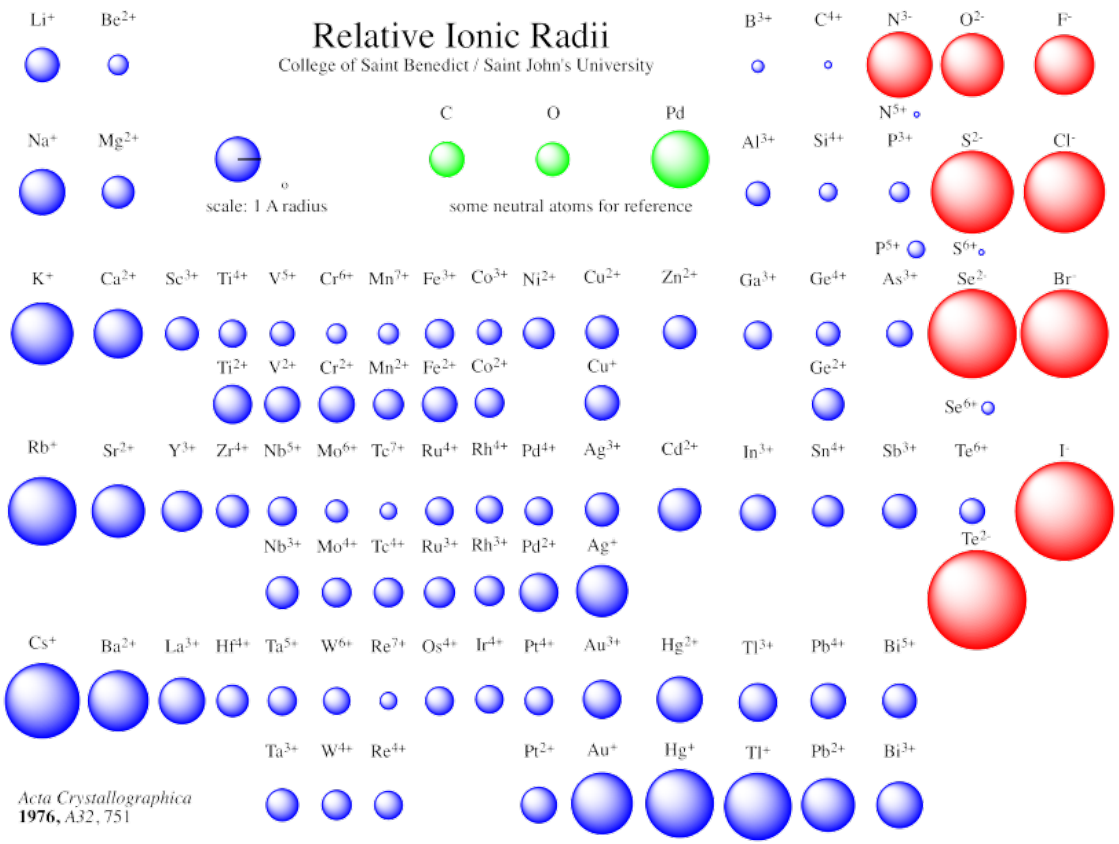

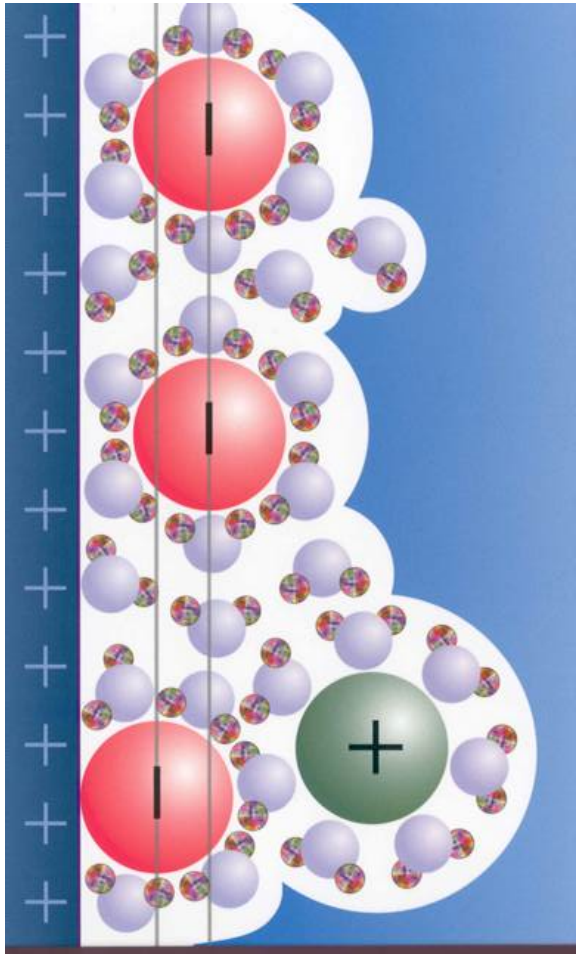

Ionic sizes vary significantly, and at high molarity, packing of ions depends significantly on solvent type, and relative sizes of counter ions.

Formulation of Solvation Energy

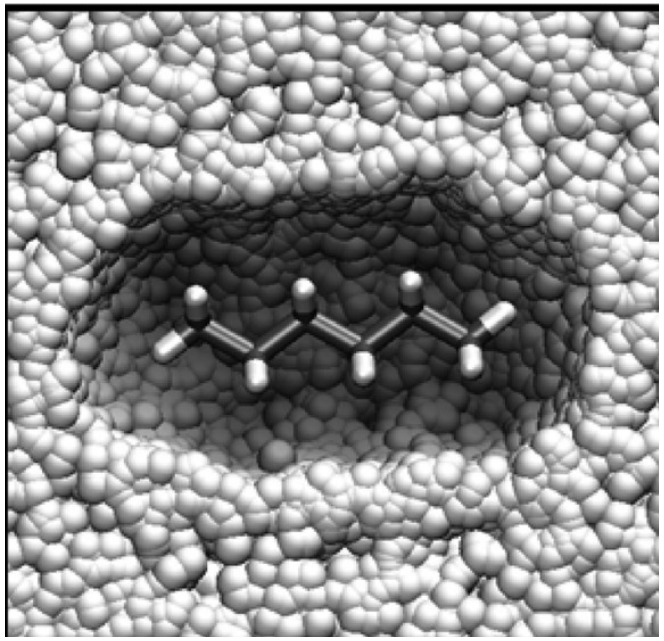

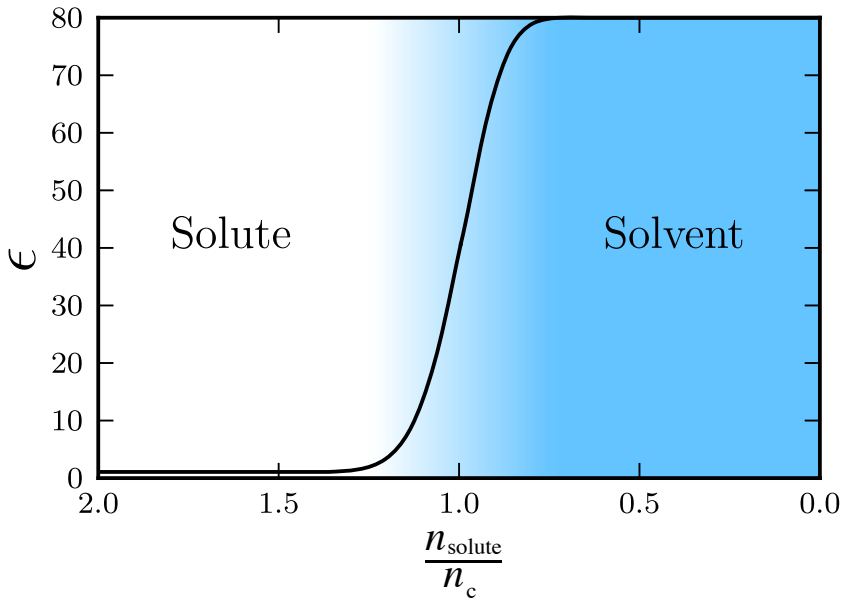

K. Mathew, R. Hennig et al, *J. Chem. Phys.*

Andreussi et al take the dielectic, $\varepsilon = \varepsilon(n_{\text{solute}})$, to be a function of the solute electronic density, with electrostatic energy

$$E^{\text{el}} = \int \varepsilon(n_{\text{solute}}) |\nabla \phi|^2 \, dx,$$

and develop a free energy by adding "quantum surface" and "quantum volume"

$$\Delta G^{\text{sol}} = \Delta G^{\text{el}} + \eta_1 S + \eta_2 V.$$

Andreussi, Dabo, Marzari, *J. Chem. Phys.* **136** (2012)

Direct Quote

"As for the remaining contributions to the solvation free energy, we have decided to treat them in a simplified way, their explicit modeling being the subject of future developments. In particular, similar to other models of solvation, the thermal motion contribution has been neglected, *while we express the sum of dispersion and repulsion free energies as a term linearly proportional to the quantum surface and the quantum volume of the molecular cavity*."

Andreussi, Dabo, Marzari, *JCP* **136** (2012).

Szostak: Primitive cell membranes

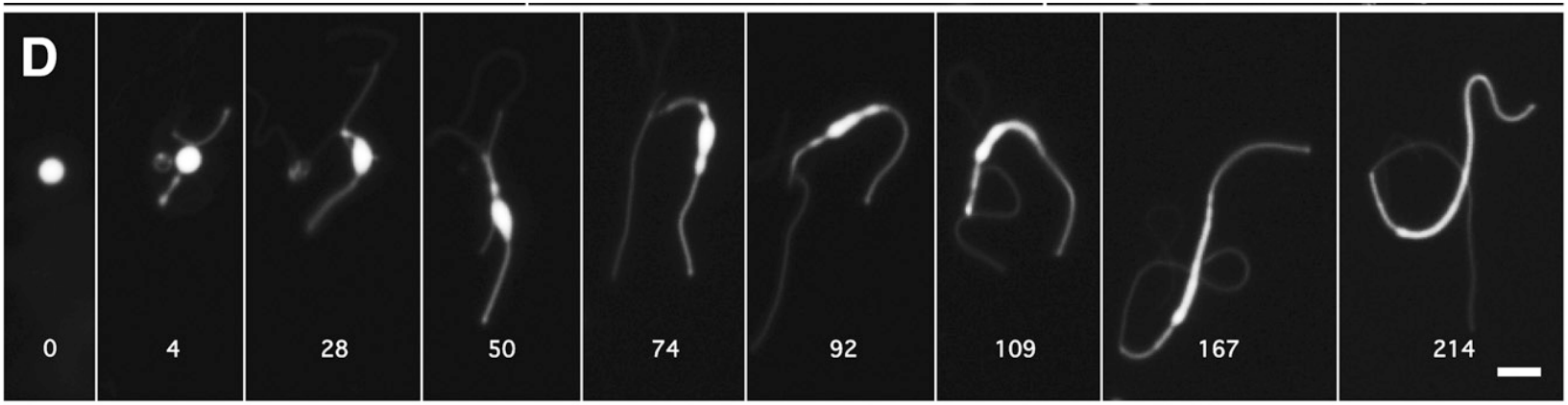

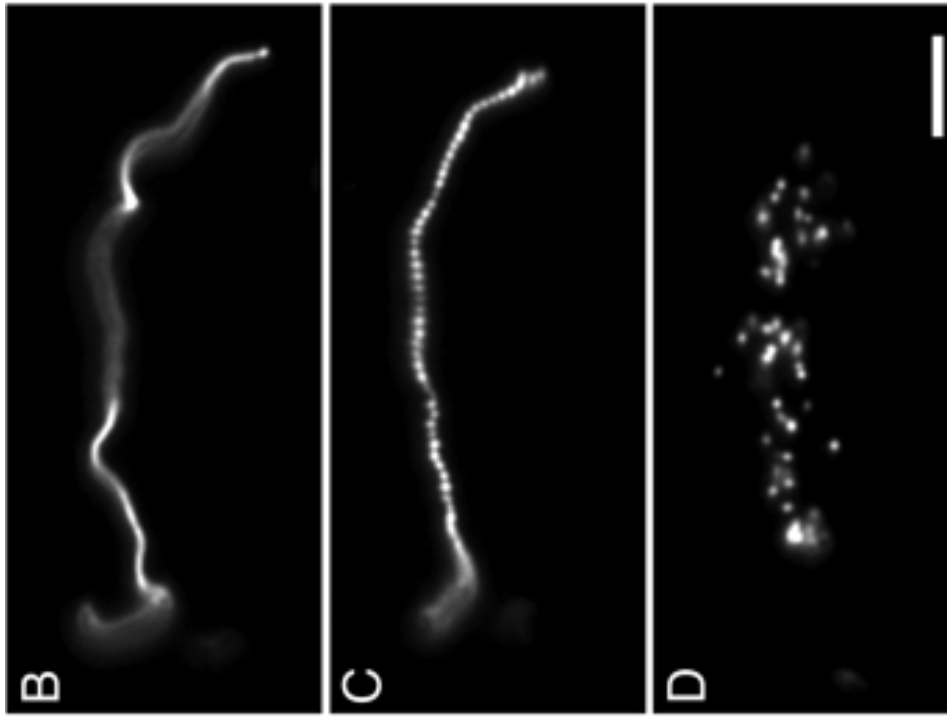

PNAS 2011/2012: primitive membranes had no phospholipids. (top) Mix 10% phospholipid membrane with pure oleate vesicles. (bottom) Radical mediated/photo-induced oxidation of thiols to disulfides induces pearling.

Cahn-Hilliard Expansion

Fix $\Omega \subset \mathbf{R}^3$, let $u \in H^1(\Omega)$ denote the volume fraction of one component of a binary mixture. Cahn and Hilliard (1958) expanded the free energy

$$\mathcal{E}(u) = \int_\Omega f(u, \epsilon^2|\nabla u|^2, \epsilon^2 \Delta u)\, dx,$$

$$= \int_\Omega f(u,0,0) + \epsilon^2 A(u)|\nabla u|^2 + \epsilon^2 B(u)\Delta u\, dx.$$

Integrating by parts on the $B(u)$ term yields the Cahn-Hilliard free energy

$$\mathcal{E}(u) = \int_\Omega \frac{\epsilon^2}{2}|\nabla u|^2 + W(u)\, dx.$$

For amphiphilic mixtures: Tuebner & Strey (1987) Gompper & Schick (1990) added higher derivatives

$$\mathcal{F}(u) := \int_\Omega f(u,0,0) + \epsilon^2 A(u)|\nabla u|^2 + \epsilon^2 B(u)\Delta u + \overbrace{C(u)}^{\geq 0} (\epsilon^2 \Delta u)^2\, dx.$$

For the primitive $\overline{A}$ of A, so that $\nabla \overline{A}(u) = A(u)\nabla u$ and integrate by parts

$$\mathcal{F}(u) := \int_\Omega f(u,0,0) + (B(u) - \overline{A}(u))\epsilon^2 \Delta u + C(u)(\epsilon^2 \Delta u)^2\, dx,$$

Complete the square

$$\mathcal{F}(u) := \int_\Omega C(u)\Big(\epsilon^2\Delta u - \overbrace{\frac{\overline{A}-B}{2C}}^{W'(u)}\Big)^2 + \overbrace{f(u) - \frac{(\overline{A}-B)^2}{C(u)}}^{P(u)}\, dx.$$

When $P \ll 1$, then the energy is very degenerate, very special.

$$\boxed{\mathcal{F}(u) = \int_\Omega \frac{1}{2}\left(\epsilon^2\Delta u - W'(u)\right)^2 + \delta P(u)\, dx.}$$

The case $\delta = 0$ was proposed as a target for Γ-convergence study by De Giorgi, it transforms all critical points of the Cahn-Hilliard free energy into global minima.

Functionalized Cahn-Hilliard Energy

An unfolding of De Giorgi's energy:

$$\mathcal{F}_{\mathrm{CH}}(u) = \int_{\Omega} \frac{1}{2}\left(\epsilon^2 \Delta u - W'(u;\tau)\right)^2 - \boxed{\epsilon^p\left(\frac{\epsilon^2\eta_1}{2}|\nabla u|^2 + \overbrace{\Pi(u)}^{\eta_2 W(u)}\right)} \, \mathrm{dx}.$$

$p = 1$ Strong Functionalization
$p = 2$ Weak Functionalization

The parameters: η_1 strength of hydrophilic portion of amphiphilic component. Pressure jump $\Pi(u)$ between phases – parameterize by η_2. Interfacial structure parameterized by "tilt" parameter τ.

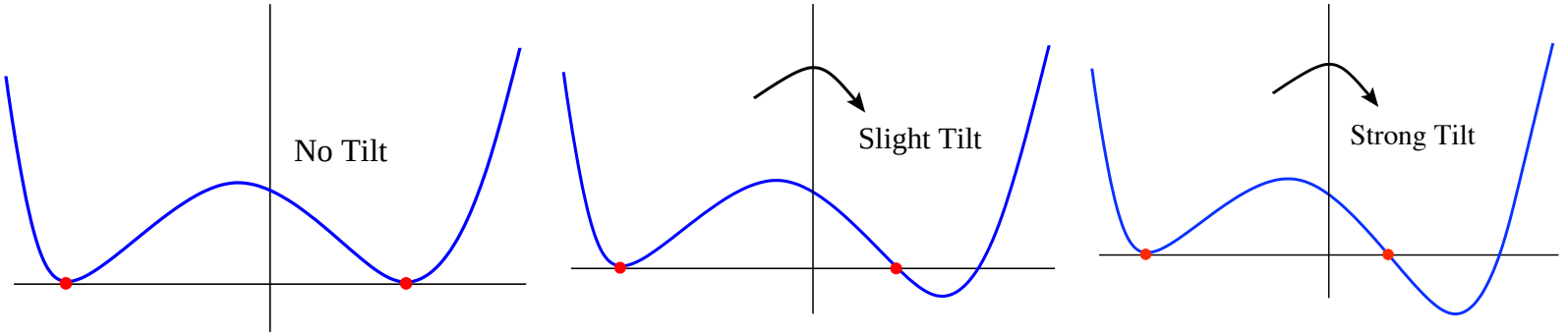

Bi-Layers: Co-Dimension One

Near a hypersurface $\Gamma \subset \mathbb{R}^n$, the Laplacian becomes

$$\epsilon^2 \Delta = \partial_z^2 + \epsilon H \partial_z + \epsilon^2 \Delta_s$$

where H is the mean curvature of the interface, and Δ_s is a surface diffusion.

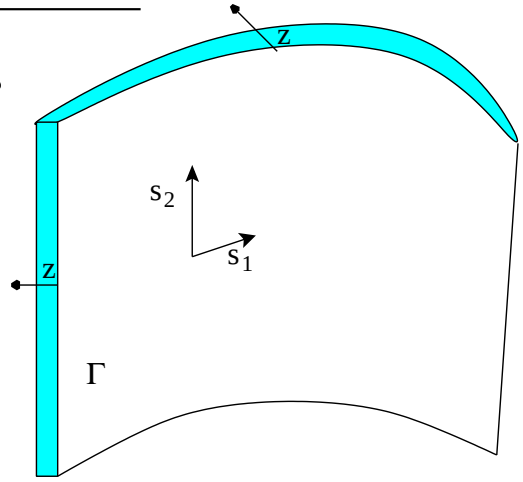

The variational derivative can be made small

$$\epsilon^2 \Delta \phi_b - W'(\phi_b) = O(\epsilon),$$

if co-dim 1 inner structure, ϕ_b, solves

$$\partial_z^2 \phi_b - W'(\phi_b) = 0.$$

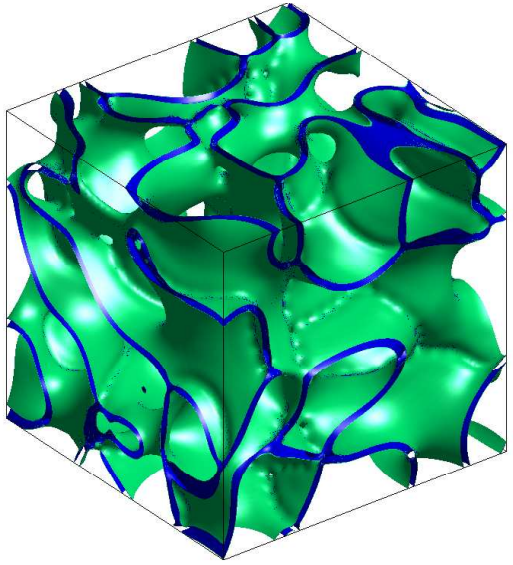

The residual of the squared-variational term is

$$\left(\epsilon^2 \Delta \phi_b - W'(\phi_b)\right)^2 =$$

$$\left(\boxed{\partial_z^2 \phi_b - W'(\phi_b)} + \epsilon H \phi_b' + \ldots\right)^2,$$

$$= \epsilon^2 \left(\phi_b(z)'\right)^2 H(s)^2.$$

Single Layer ≠ Bilayer

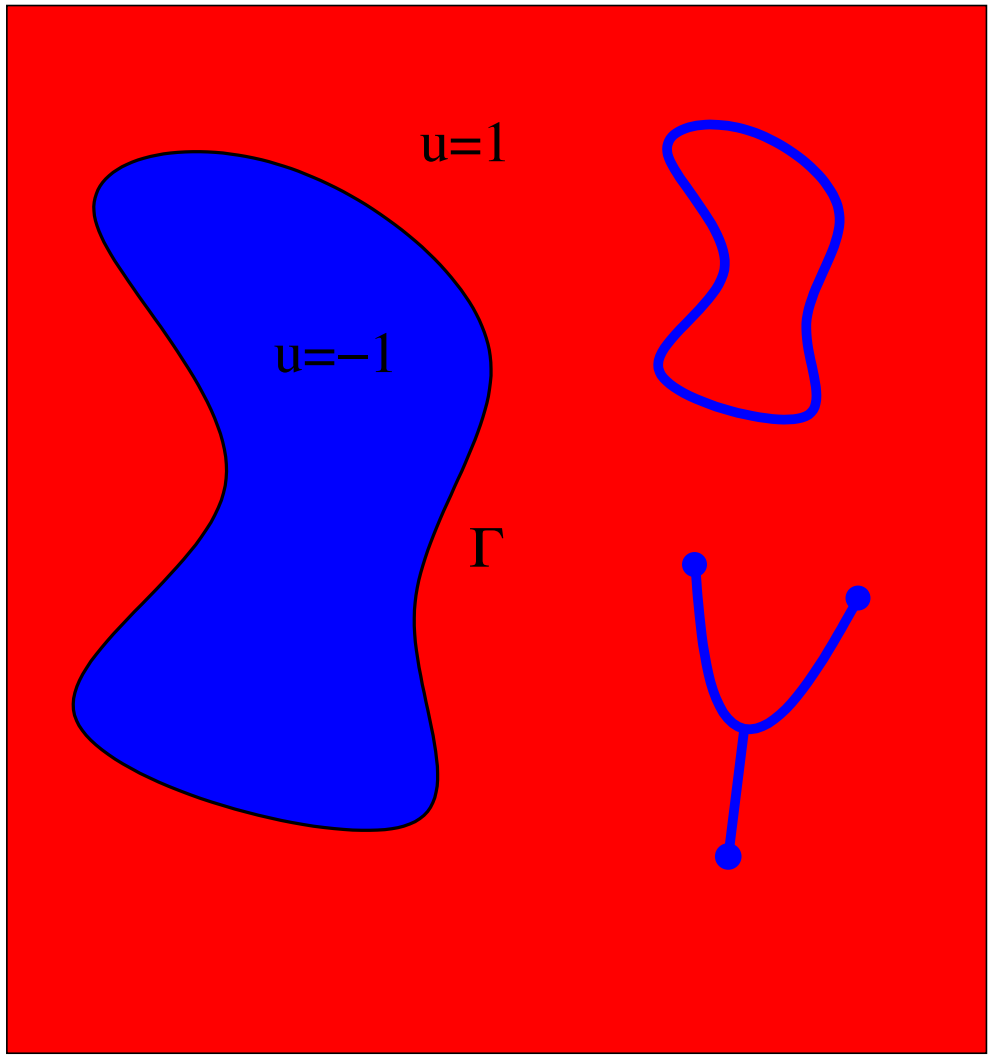

Bilayers can open holes, modulate their width, and naturally form end-cap defects.

Pores: Co-Dimension Two

Fix $\Gamma \subset \mathbb{R}^3$, a cylindrical geometry leads to (R, θ, s) variables and the decomposition

$$\epsilon^2 \Delta = \Delta_R - \begin{pmatrix} \kappa_1 \\ \kappa_2 \end{pmatrix} \cdot \begin{pmatrix} \partial_{z_1} \\ \partial_{z_2} \end{pmatrix} + \epsilon^2 D_s^2.$$

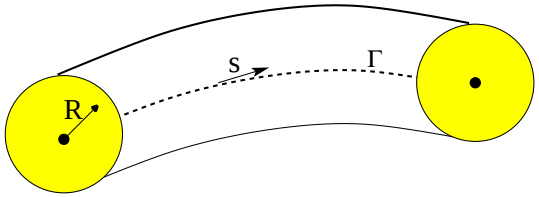

With angular symmetry, the co-dim 2 inner structure satisfies

$$\partial_R^2 \phi_2 + \frac{1}{R} \partial_R \phi_p = W'(\phi_p),$$

where (R, θ) are polar versions of (z_1, z_2). The squared-variational remainder is

$$\left(\epsilon^2 \Delta \phi_p - W'(\phi_p)\right)^2 = \epsilon^2 \left(\phi_p'\right)^2 |\kappa|^2.$$

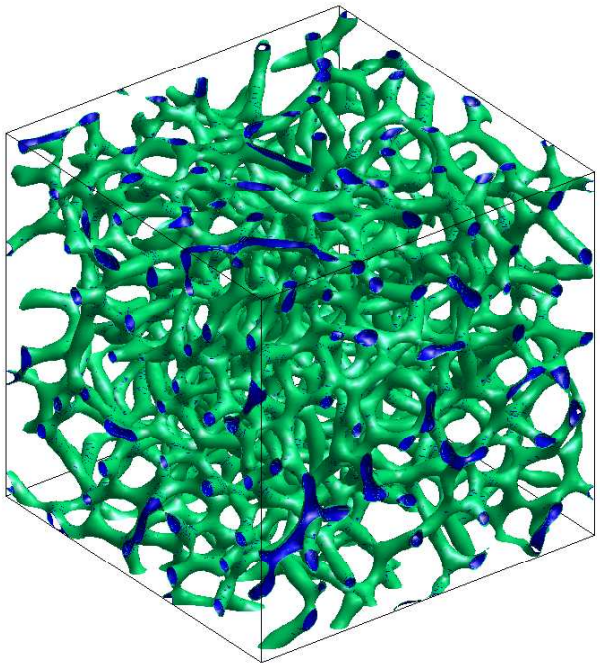

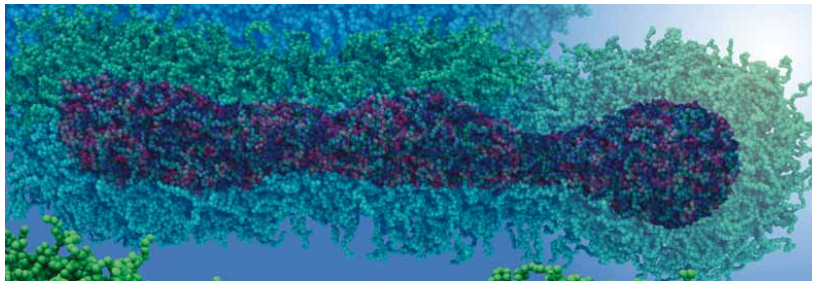

Loverde, Macromolecules 2010

Morphological Competition

$$\mathcal{F}_{\mathrm{CH}}(u) = \int_\Omega \frac{1}{2}\left(\epsilon^2 \Delta u - W'(u)\right)^2 - \epsilon^p \left(\frac{\eta_1}{2}\epsilon^2 |\nabla u|^2 + \eta_2 W(u)\right) dx.$$

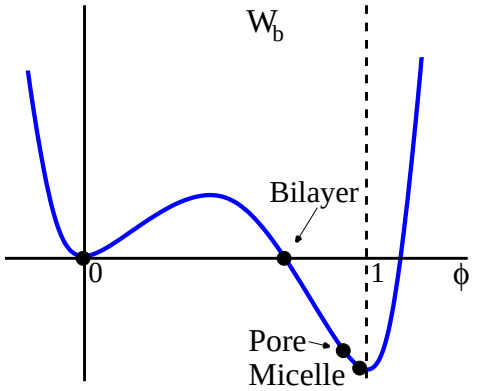

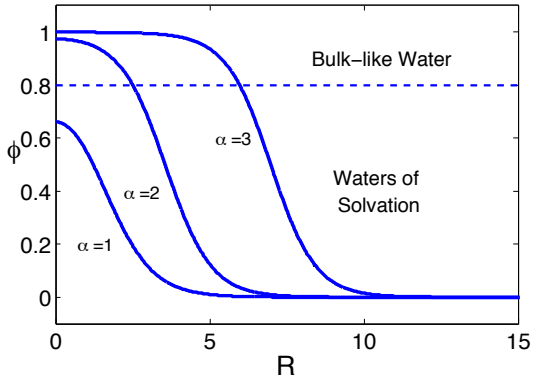

Co-dim 1	$\partial_z^2 \phi_b = W'(\phi_b)$	$\int_\Omega W(\phi_b)\, dx > 0$
Co-dim 2	$\frac{1}{R}\partial_R(R\partial_R)\phi_p = W'(\phi_p)$	$\int_\Omega W(\phi_p)\, dx = 0$
Co-dim 3	$\frac{1}{R^2}\partial_R(R^2\partial_R)\phi_m = W'(\phi_m)$	$\int_\Omega W(\phi_m)\, dx < 0.$

Impact of Volume Term

$$\mathcal{F}_{\mathrm{CH}}(u) = \int_{\Omega} \frac{1}{2}\left(\epsilon^2 \Delta u - W'(u)\right)^2 - \epsilon^p \left(\frac{\eta_1}{2}\epsilon^2 |\nabla u|^2 + \eta_2 W(u)\right) dx.$$

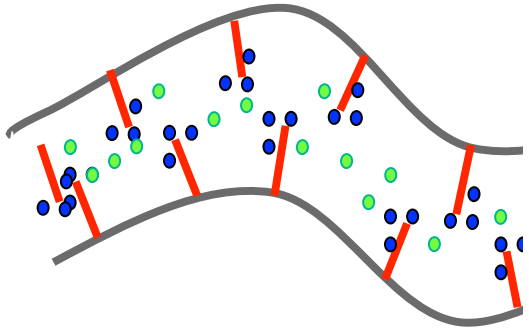

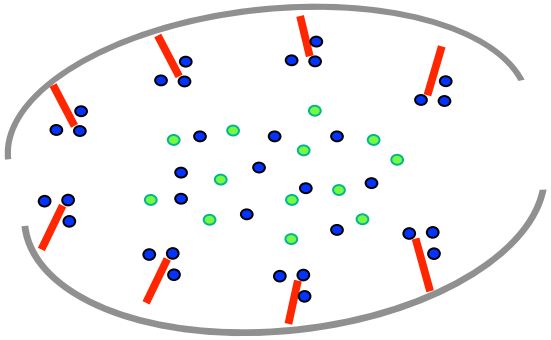

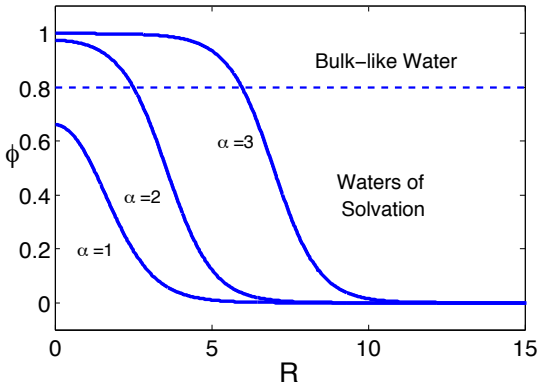

For pores in Nafion, the parameter η_2 could express the counter-ion's (protons) preference for bulk-like water verses waters of solvation.

Key Prediction: A preference for bulk-like water selects pores over bilayers and selects micelles over pores.

M_n^{core} (g/mol)	2500 ± 40	5850 ± 204
bilayer	8.7 ± 1.2	15.8 ± 2.8
cylinder	14.3 ± 1.6	25.4 ± 3.3
sphere (nm)	18.4 ± 2.6	38.8 ± 10.2

Jain and Bates, *Macromolecules* (2004)

Small Sample of Parameter Space $\tau = -0.4$, $\epsilon = 0.03$

$$u_t = \Delta \frac{\delta \mathcal{F}_{\mathrm{CH}}}{\delta u} \quad \Longrightarrow \quad \frac{d}{dt}\mathcal{F}_{\mathrm{CH}}(u) \leq 0$$

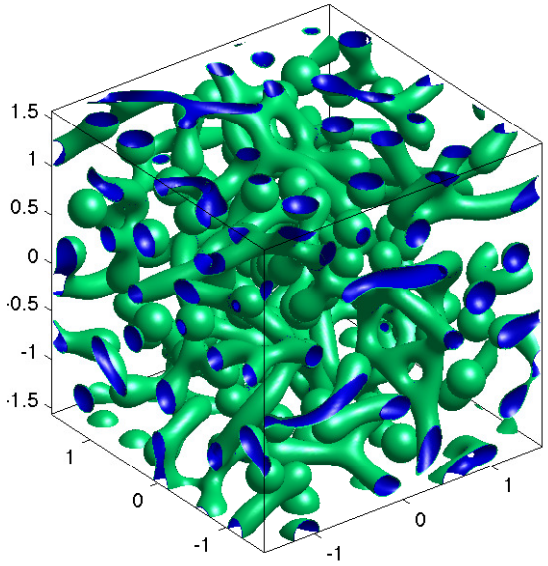

$\eta_2 = -2$
Micelles - Pores
Co-dim 2 & 3

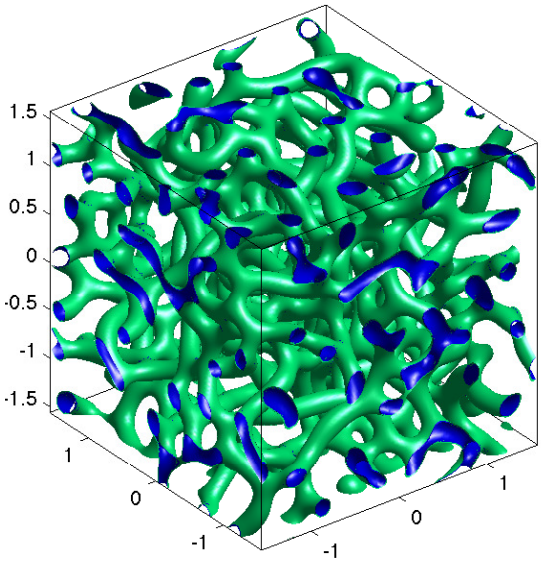

$\eta_2 = 1$
Pore Network
Co-dim 2

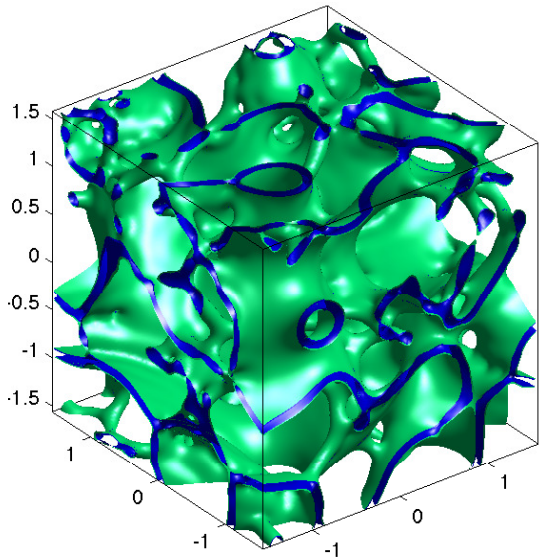

$\eta_2 = 3$
Bilayers
Co-dim 1

Identical, randomly ± 1 initial data. Co-dimension = choice of inner structure.

Experimental Morphology

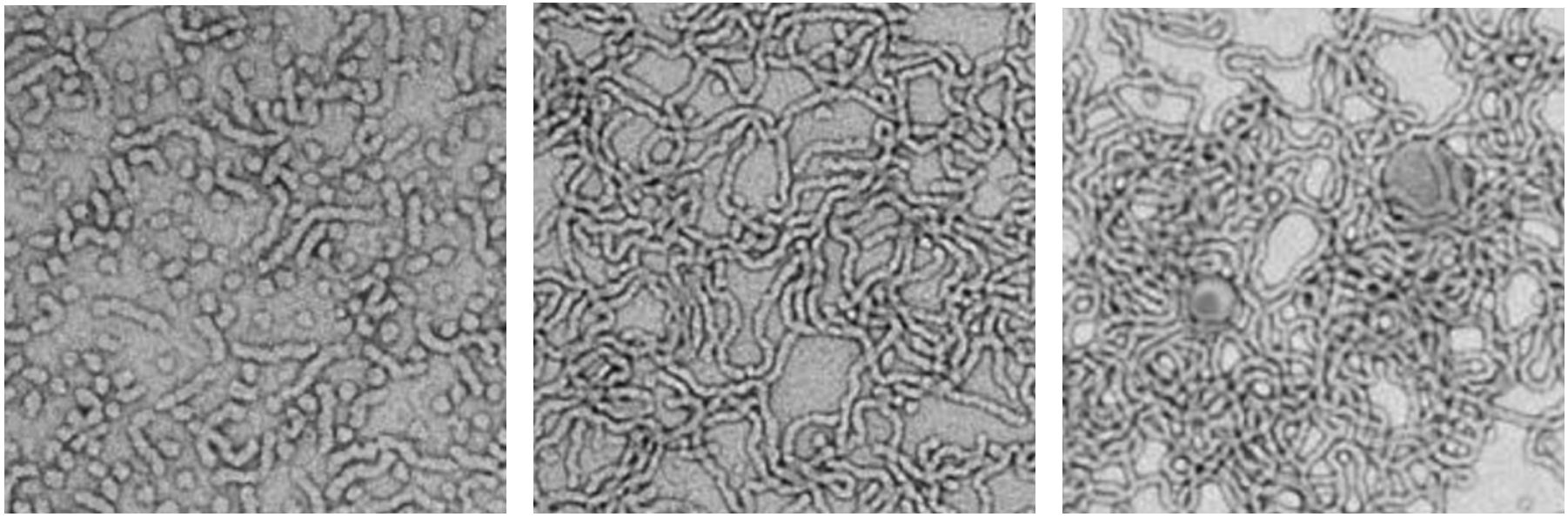

Blends of amphiphilic diblock copolymers with fixed lengths of hydrophilic block and differing lengths of hydrophobic chain. The diblocks with the longest hydrophobic chains from coexisting micelle/worm structures, while decreasing hydrophobic chain length leads to worm only, and coexisting worm/bilayer (hollow) vesicles.
L. Ratcliffe, A. Ryan, and S. Armes, *Macromolecules* **46** (2013).

Bifurcation Diagram

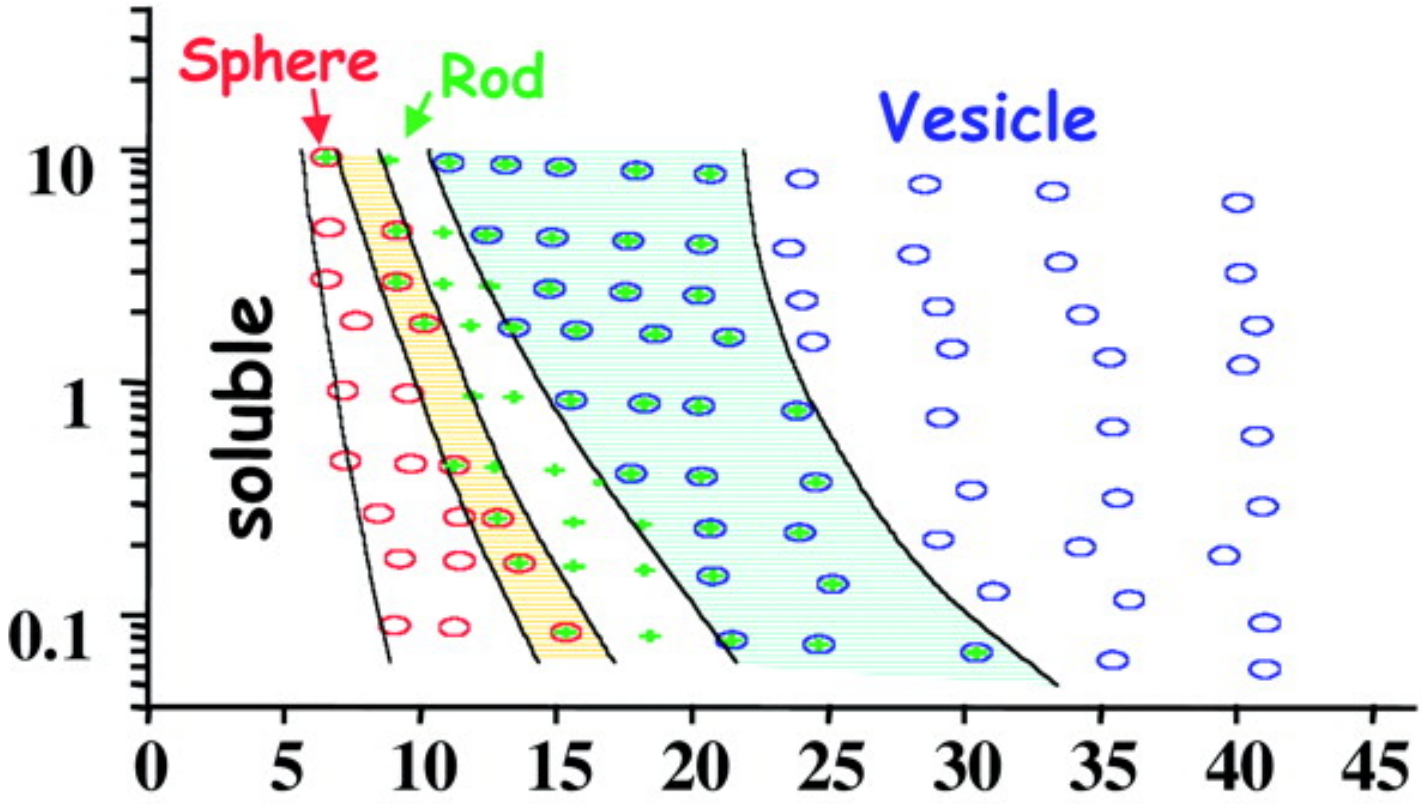

Bifurcation diagram for amphiphilic copolymers as function of weight percent of copolymer (vertical log axis) and water volume fraction within water-dioxane solvent blend (horizontal axis). Increasing water fraction drives bifurcations from micelle (sphere) to pore (rod) to bilayer (vesicle), shaded regions indicate pearling and co-existence, from D. Dicher and A. Eisenberg, *Science* **297** (2002).

Merging of Dumb-bell Structures into Pore Network

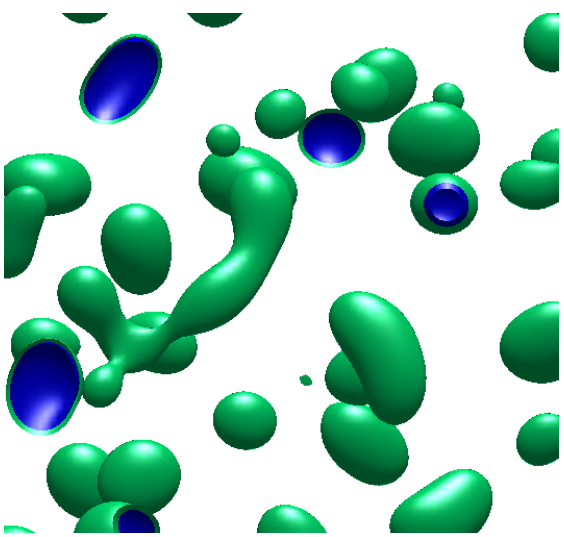

(a)

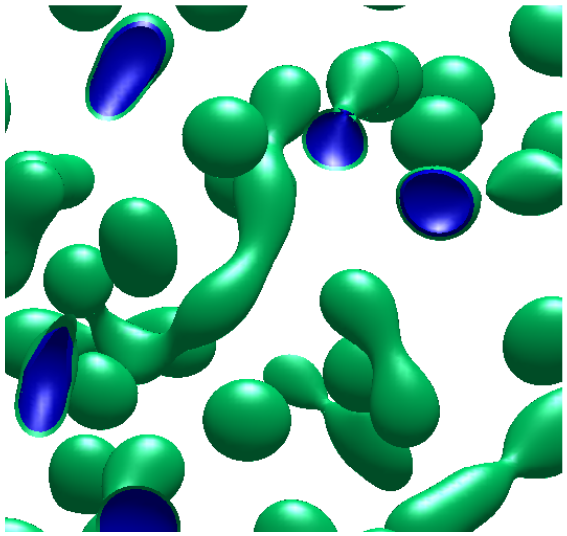

(b)

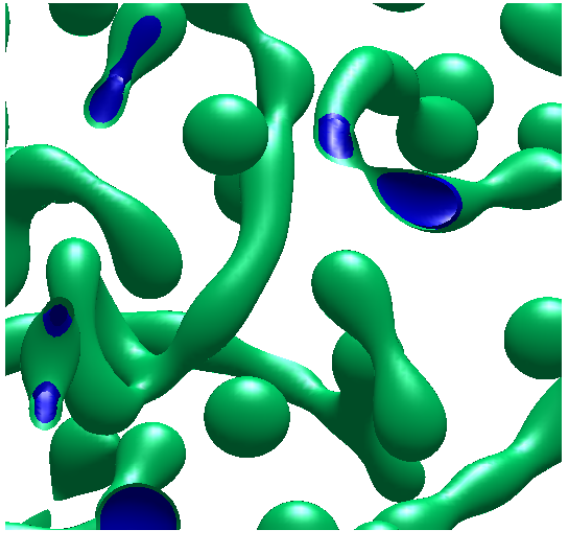

(c)

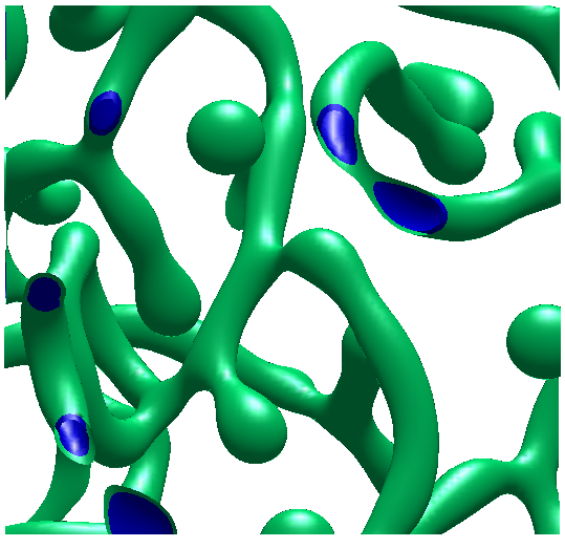

(a) Random initial data coarsens into micelles,
(b) over-sized micelles are unstable and grow into dumb-bells,
(c-d) dumb-bells elongate, merge and form a pore network.

Spectra of Functionalized Bilayers

For strong functionalization the bilayer dressing of hypersurface Γ:

$$u_b(x) = \phi_b(z) + \epsilon(\gamma_1 + \phi_{1,\mathrm{loc}}(z)) + O(\epsilon^2)$$

Stability of bilayers is determined by the eigenvalues of the second variation

$$\mathbb{L} := \frac{\delta^2 \mathcal{F}}{\delta u^2}(u_b),$$

$$= \boxed{(\partial_z^2 - W''(\phi_b) + \epsilon^2 \Delta_s)^2} + O(\epsilon),$$

whose eigenfunctions separate to $O(\epsilon)$,

$$\Psi_{j,n} = \psi_j(z)\Theta_n(s) + O(\epsilon).$$

Instability can come from pearling (ground-state ψ_0 with $\lambda_0 > 0$) or meander eigenvalues ($\psi_1 = \phi_b'$ with $\lambda_1 = 0$).

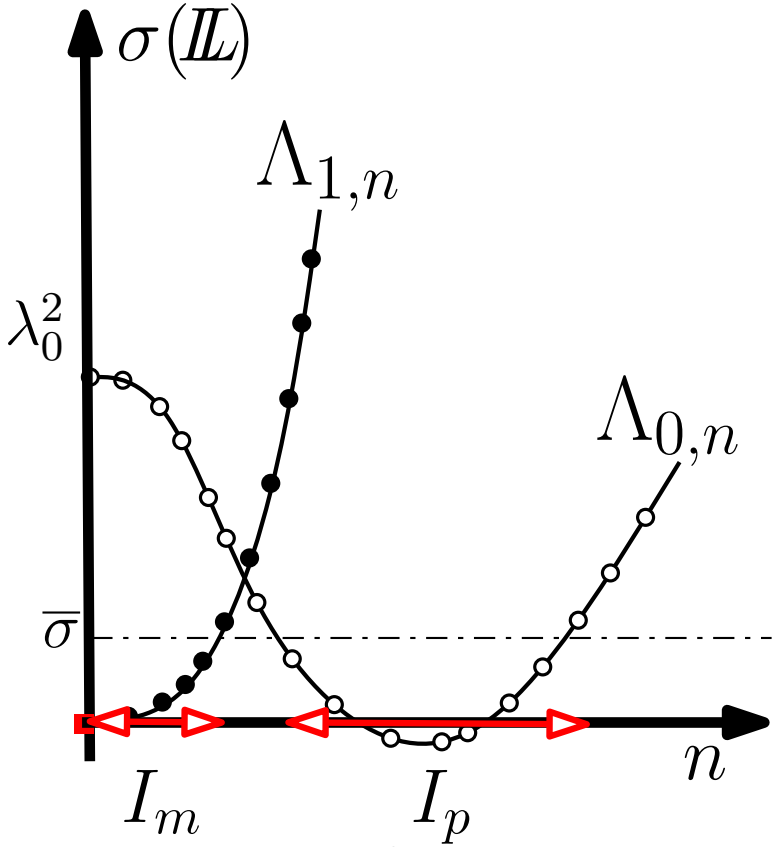

$$\Lambda_{0,n} = (\lambda_0 - \epsilon^2 \beta_n)^2 + \epsilon[\lambda_0(\eta_1 - \eta_2) - \gamma_1 S] + O(\epsilon^2).$$

The sign of $S = \int_{\mathbb{R}} W'''(\phi_b)\psi_0^2(z)\, dz$ determines if pearling absorbs or liberates lipids, connecting background level γ_1 to the pearling bifurcation.

Functionalization = Swift-Hohenbergization

Recipe for Functionalized Spectra in co-dim 1:Hayrapetyan & P., ZAMP (2014)
Unstable 1D eigenvalues generate "Swift-Hohenberg" spectrum in the FCH.

$$\mathbf{1D-inner} \qquad \mathbb{R}^n \qquad \mathbf{Functionalized}$$

$$L_0 = \partial_z^2 - W''(\phi_b) \mapsto L = L_0 + \epsilon^2 \Delta_s \mapsto \mathbb{L} = -L^2 + O(\epsilon)$$

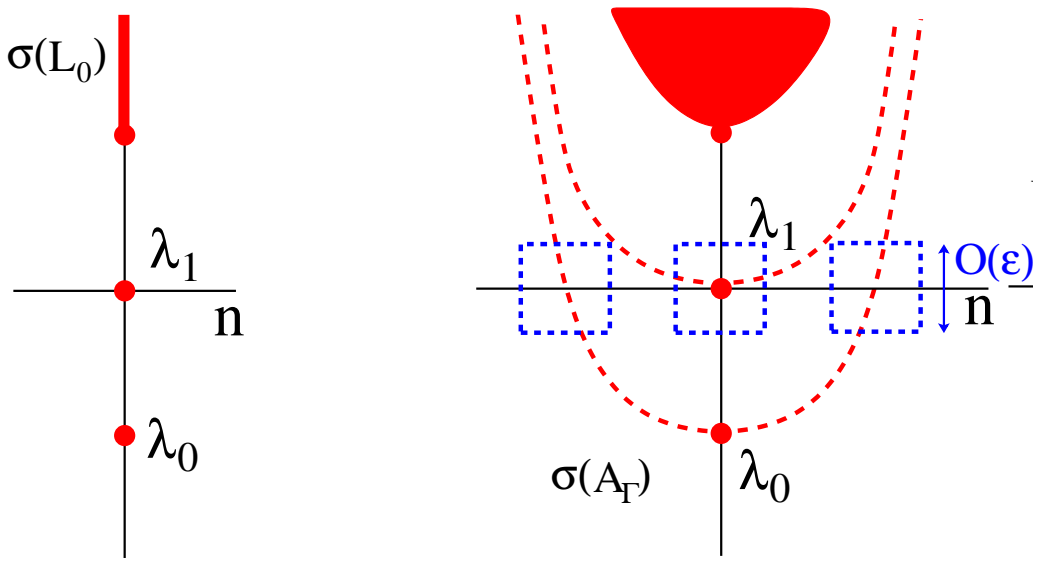

Pearling Spectra for Strongly Functionalized Bilayers

Theorem: (Kraitzman, K.P.) Fix $\gamma_2 \in \mathbb{R}$ and $\Gamma \subset \mathbb{R}^d$ a smooth, closed, co-dim one interface which is far from self-intersection, and let

$$u_b(x) = \phi_b(z) + \epsilon(\gamma_1 + \phi_{1,\text{loc}}(z)) + O(\epsilon^2)$$

be the associated quasi-steady bilayer interface with far-field values

$$\lim_{z\to\pm\infty} u_b(z,s) = b_- + \epsilon\gamma_1 + O(\epsilon^2).$$

Then the only unstable eigenvalues associated to $\mathbb{L}$ arise from pearling or meander eigenvalues. Moreover there exists $N \sim \epsilon^{-\nu}$ such that all $O(\epsilon)$ pearling eigenvalues are approximated by the eigenvalues of the matrix $\mathrm{M} \in \mathbb{R}^{N\times N}$

$$\mathrm{M}_{ij} = \delta_{ij}\Big[((\lambda_0 - \epsilon^2\beta_n)^2 + \epsilon[\lambda_0(\eta_1 - \eta_2) - \gamma_1 S]\Big] \\ -2\epsilon^2\langle H^2, \Theta_i\Theta_j\rangle_\Gamma \|\psi_0'\|_2^2 + O(\epsilon^3).$$

In particular stability to pearling depends upon the far-field value, γ_1, the value of $\eta_1 - \eta_2$, and the mean curvature $H = H(s)$ of Γ.

If $H \in H^4(\Gamma)$ then curvature effects perturb diagonal terms, if $H \notin H^4(\Gamma)$, then curvature effects are potentially dominant – implying loss of Canham-Helfrich.

Numerical Validation: Initial data bilayer is too wide.

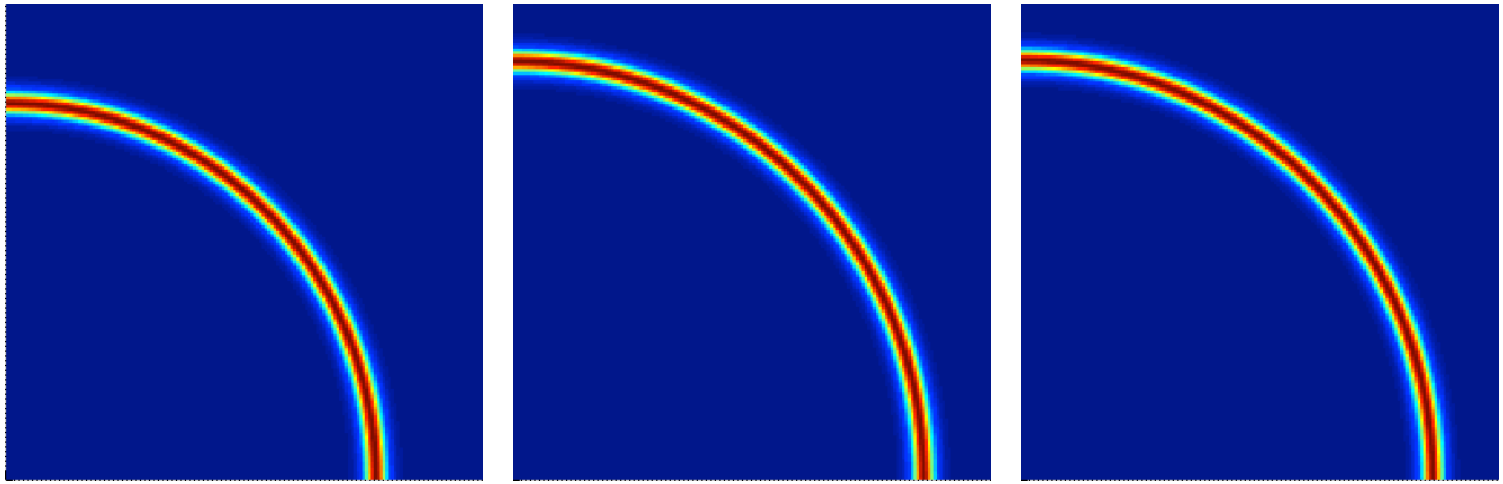

Images for $\epsilon = 0.1$, $\eta_1 = 1$, and $\eta_2 = 2$ at times $t = 0$, $t = 857$, and $t = 3000$. No pearling, convergence to equilibrium on the $O(\epsilon^{-3})$ time-scale.

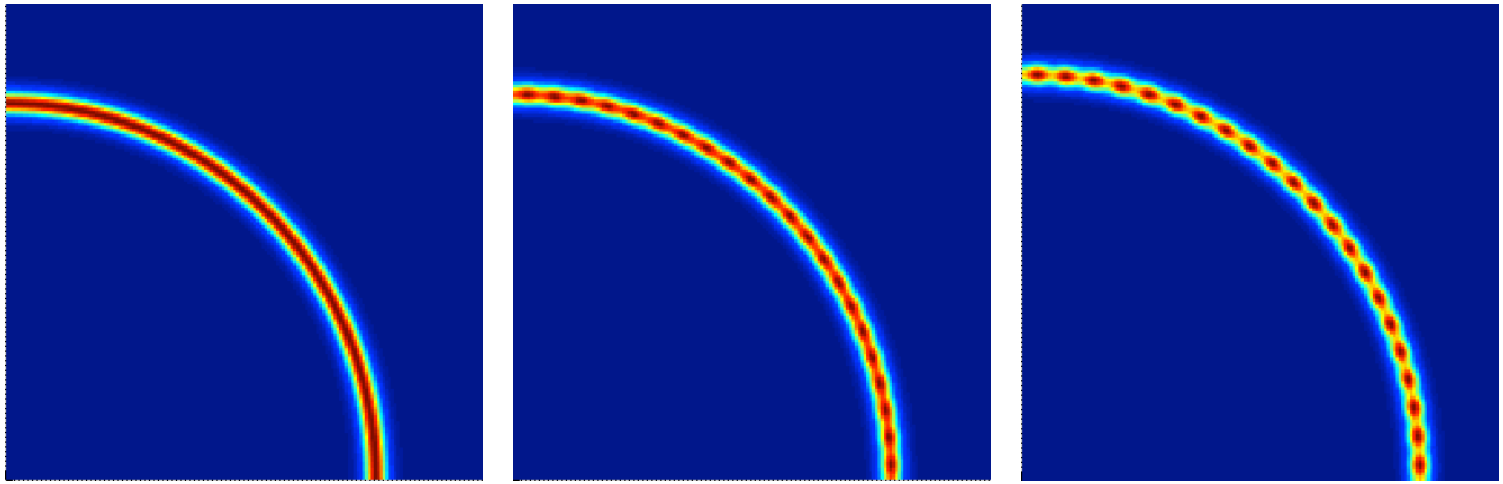

(Szostak) $\epsilon = 0.1$, $\eta_1 = \eta_2 = 2$ at times $t = 0$, $t = 114$, and $t = 804$.

Rigorous Existence of Pearled Bilayers (with Q. Wu)

Construct small-amplitude, pearled solutions of the strong FCH equilibrium in $\mathbb{R}^2$

$$\left(\partial_z^2 - W''(u) + \epsilon^2\partial_s^2 + \epsilon\eta_1\right)\left(\partial_z^2 u - W'(u) + \epsilon^2\partial_s^2 u\right) + \epsilon\eta_2 W'(u) = \epsilon\gamma.$$

The spatial dynamics approach writes this as a first-order four-dimensional system

$$\partial_s U = \mathbb{L}U + \mathbb{F}(U),$$

and projects onto the eight-dimensional center space (4-pearling/4-meander) of $\mathbb{L}$.

The reversibility and structure of the FCH lead to the 1:1 resonant normal form. Truncated to cubic order in the pearling subspace yields a 4-dim ODE

$$\dot{C}_1 = C_2 + iC_1\left[\omega_0 + \alpha_7|C_1|^2 + i\alpha_8\kappa\right],$$

$$\dot{C}_2 = C_1\left[-\frac{\mu_5}{2\lambda_0}\epsilon + \alpha_1|C_1|^2 + i\alpha_2\kappa\right] + iC_2\left[|C_1|^2 + i\alpha_8\kappa\right],$$

where the conserved quantity $\kappa = C_1\overline{C}_2 - \overline{C}_1 C_2$. The system uncouples to a 2nd order scalar system for the real r_1 under the transformation

$$C_1(s) = \sqrt{\epsilon}r_1 e^{i(\omega s+\theta)},$$

$$C_2(s) = \epsilon r_2 e^{i(\omega s+\theta)}.$$

Degeneracy of Circular, Pearled Bilayers

Assume $\Omega \subset \mathbb{R}^2$. Fix $\eta_1, \eta_2 \in \mathbb{R}$ and $R_- > 0$. Assume that W is a non-degenerate double well potential and that

$$\alpha_0 = -\gamma_1 S + \lambda_0(\eta_1 - \eta_2) > 0.$$

Then, subject to a non-degeneracy condition then there exist positive constants $\varepsilon_0 > 0$, $\kappa_0 > 0$, and $n_- > 0$ such that, for all $\varepsilon \in (0, \varepsilon_0]$ and each

$$\mathrm{n} \in \mathbb{Z}^+ \cap [n_-/\varepsilon, +\infty),$$

the stationary FCH admits a smooth one-parameter family of circular pearled solutions, parameterized by $\kappa \in [-\kappa_0, \kappa_0]$.

$$u_{\mathrm{p,n}}(\theta, r; \sqrt{|\kappa|}) = u_h(r) + 2\frac{\sqrt{\varepsilon|\kappa|}}{\sqrt[4]{\alpha_0}} \cos(\mathrm{n}\theta)\psi_0(r) + \mathcal{O}\left(\varepsilon(\sqrt{\varepsilon} + \sqrt{|\kappa|})\right),$$

where the radius of the circular bilayer

$$R_{0,\mathrm{n}} = \mathrm{n}\varepsilon\left[1 - \sqrt{\alpha_0\varepsilon} + \mathcal{O}\left(\varepsilon(1 + \sqrt{|\kappa|})\right)\right].$$

depends only weakly upon κ. The far-field limit of the extended pearled solution

$$\lim_{r\to\infty} u_{\mathrm{p,n}}(\theta, r) = \lim_{r\to\infty} u_h(r) = u_-(\varepsilon),$$

is independent of n. [$\mathcal{O}(\epsilon^2)$ pert to background $\mathcal{O}(\sqrt{\epsilon})$ pert to amp.]

Bifurcation Analysis – Szostak

For generic bilayers (arb Γ_b and $S > 0$) pearling occurs if

$$\gamma_1 < A_p(\tau)(\eta_1 - \eta_2),$$

while spherical bilayers are unstable to meander instability ("fingering") if

$$\gamma_1 > A_m(\tau)(\eta_1 + \eta_2).$$

Increasing γ_1 (adding free lipids to background) induces fingering

Increasing η_1 (photo-induced oxidation of thiols) leads to pearling

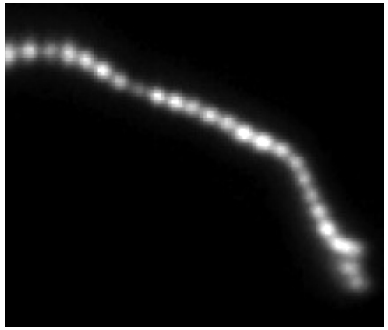

Geometric Evolution of Bilayers: Meander CM reduction

$$u_t = -\Delta \frac{\delta \mathcal{F}}{\delta u},$$

At $t_1 = \epsilon t$, for a bilayer Γ we obtain the Mullins-Sekerka flow for γ_1:

$$\begin{array}{rcll} \Delta\gamma_1 & = & 0, & \text{in } \Omega\backslash\Gamma, \\ \gamma_1 & = & c(t_1) + H\phi_b'(0), & \text{on } \Gamma, \\ [\![\partial_n \gamma_1]\!] & = & 0 & \text{on } \Gamma, \end{array}$$

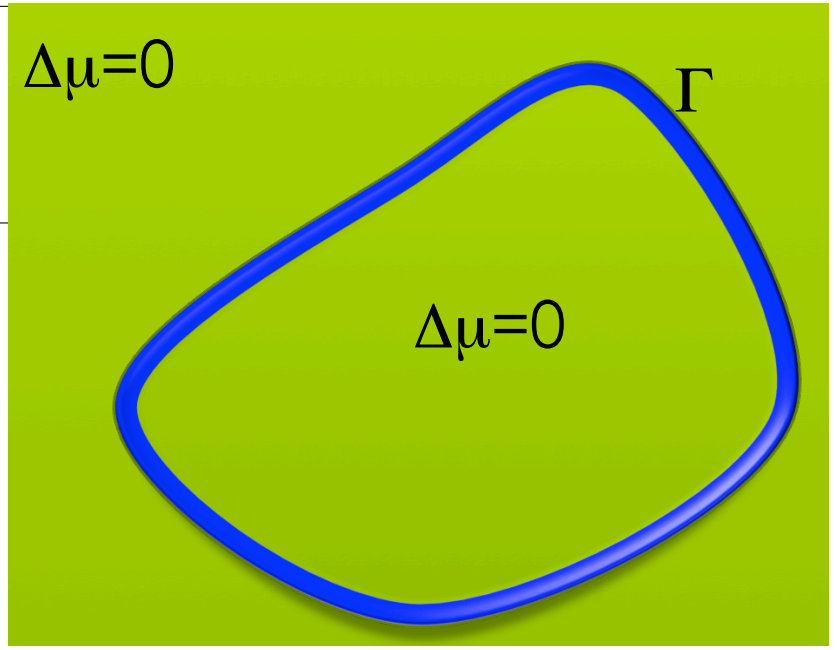

with normal velocity

$$V_b = \partial_n \gamma_1^- - (\gamma_1 - \gamma_p(\tau))H.$$

However, $\phi_b'(0) = 0$ and the background Lipid level γ_1 is spatially constant. Combined with conservation of mass we obtain the coupled system

$$V_b = (\gamma_1 - \gamma_b(\tau))H,$$

$$\gamma_1'(t_1) = -(\gamma_1(t_1) - \gamma_b) \int_\Gamma H^2(s)\, ds.$$

The coupled system *prevents* singularity by driving $\gamma_1 \to \gamma_b$.

Coupled Geometric Evolution of Bilayers and Pores

For pores we derive the normal velocity $\vec{\mathbf{V}}_p$ of its co-dimension two curve $\boldsymbol{\Gamma}_p$,

$$\vec{\mathbf{V}}_p = (\gamma_1 - \gamma_p(\tau))\vec{\kappa},$$

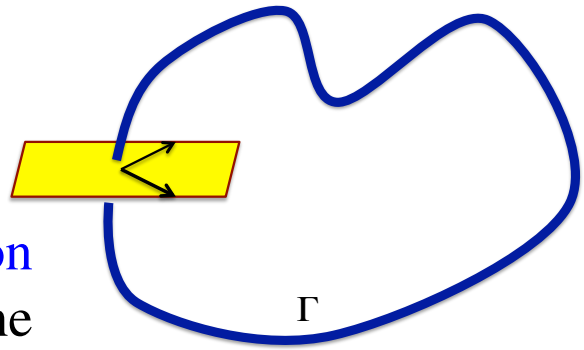

For co-existing bilayers and pores, the common value of the far-field lipid density, γ, couples the evolution of the two morphologies:

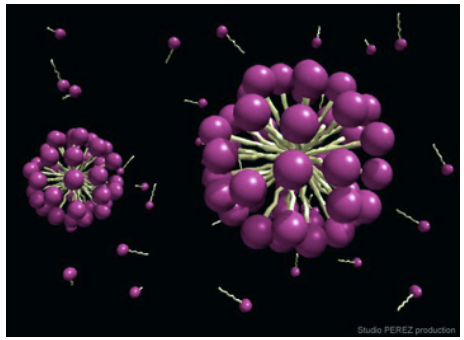

$$\begin{aligned} \boldsymbol{V_n} &= (\gamma_1 - \gamma_p(\tau))\boldsymbol{H} \\ \vec{\mathbf{V}}_p &= (\gamma_1 - \gamma_p(\tau))\vec{\kappa} \\ \frac{\boldsymbol{d\gamma_1}}{\boldsymbol{dt_1}} &= -(\gamma_1 - \gamma_p)\int_{\Gamma_b} \boldsymbol{H^2 dS} + \\ &\qquad -\epsilon(\gamma_1 - \gamma_p)\int_{\Gamma_p} |\vec{\kappa}|^2\, \boldsymbol{ds}. \end{aligned}$$

Relative size of $\gamma_p(\tau)$, $\gamma_b(\tau)$, and the pearling point $\boldsymbol{A_p}(\tau)(\eta_1 - \eta_2)$ is crucial to dynamics.

Coupled Geometric Evolution of Bilayers and Pores

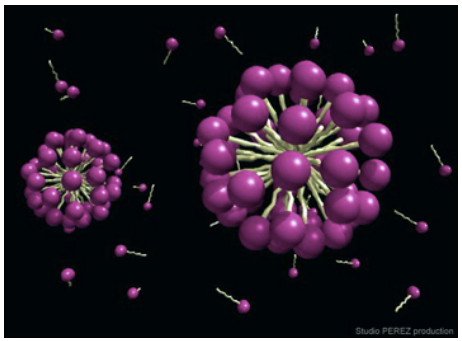

$$V_n = (\gamma_1 - \gamma_p(\tau))H$$
$$\vec{V}_p = (\gamma_1 - \gamma_p(\tau))\vec{\kappa}$$
$$\frac{d\gamma_1}{dt_1} = -(\gamma_1 - \gamma_p)\int_{\Gamma_b} H^2 dS + - \epsilon(\gamma_1 - \gamma_p)\int_{\Gamma_p} |\vec{\kappa}|^2 \, ds.$$

Relative size of $\gamma_p(\tau)$, $\gamma_b(\tau)$, and the pearling point $A_p(\tau)(\eta_1 - \eta_2)$ is crucial to dynamics.

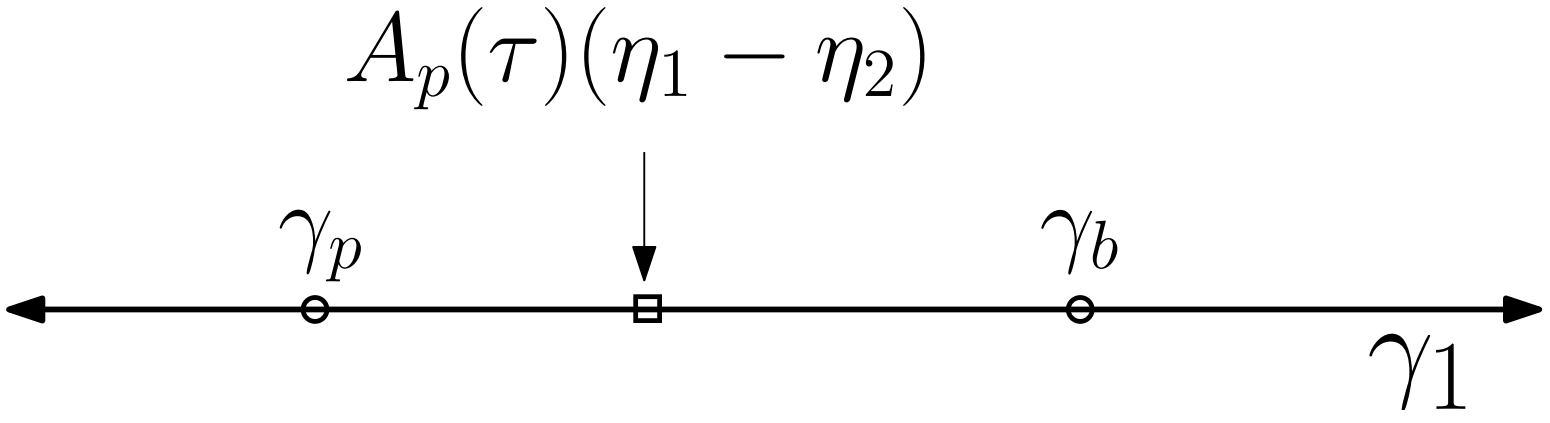

Coupled Geometric Evolution of Bilayers and Pores

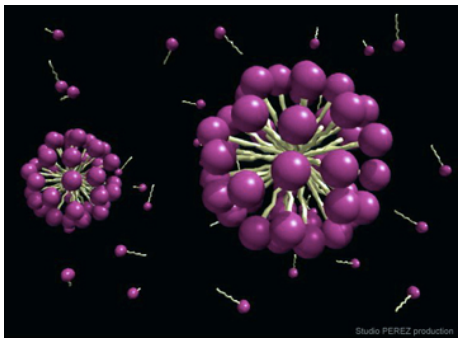

$$V_n = (\gamma_1 - \gamma_p(\tau))H$$
$$\vec{V}_p = (\gamma_1 - \gamma_p(\tau))\vec{\kappa}$$
$$\frac{d\gamma_1}{dt_1} = -(\gamma_1 - \gamma_p)\int_{\Gamma_b} H^2 dS + - \epsilon(\gamma_1 - \gamma_p)\int_{\Gamma_p} |\vec{\kappa}|^2 \, ds.$$

Relative size of $\gamma_p(\tau)$, $\gamma_b(\tau)$, and the pearling point $A_p(\tau)(\eta_1 - \eta_2)$ is crucial to dynamics.

$$A_p(\tau)(\eta_1 - \eta_2)$$

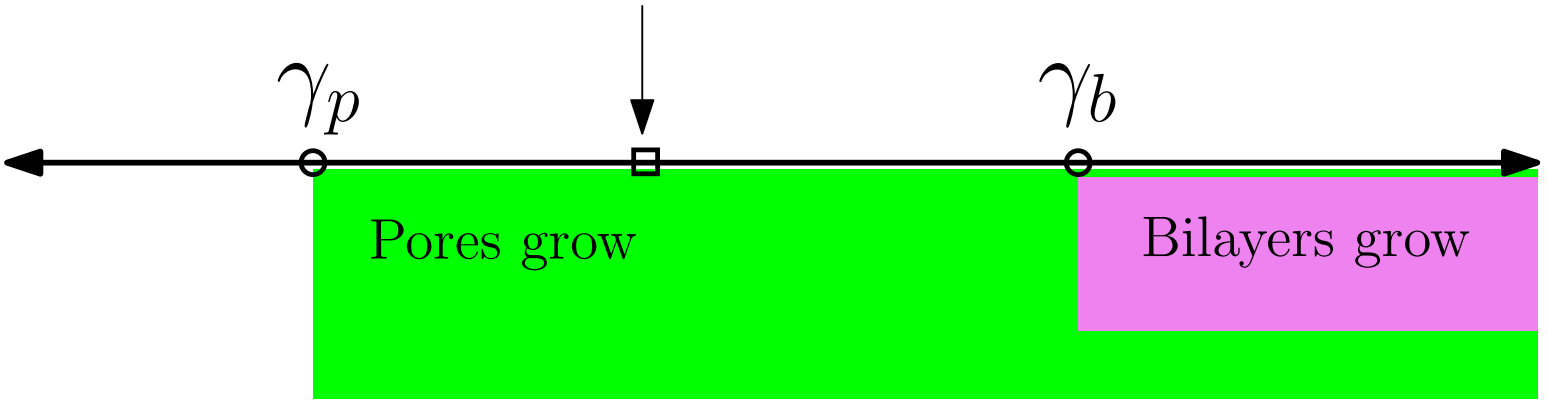

Coupled Geometric Evolution of Bilayers and Pores

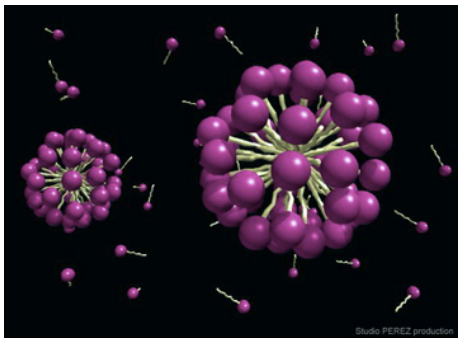

$$V_n = (\gamma_1 - \gamma_p(\tau))H$$
$$\vec{V}_p = (\gamma_1 - \gamma_p(\tau))\vec{\kappa}$$
$$\frac{d\gamma_1}{dt_1} = -(\gamma_1 - \gamma_p)\int_{\Gamma_b} H^2 dS + - \epsilon(\gamma_1 - \gamma_p)\int_{\Gamma_p} |\vec{\kappa}|^2 \, ds.$$

Relative size of $\gamma_p(\tau)$, $\gamma_b(\tau)$, and the pearling point $A_p(\tau)(\eta_1 - \eta_2)$ is crucial to dynamics.

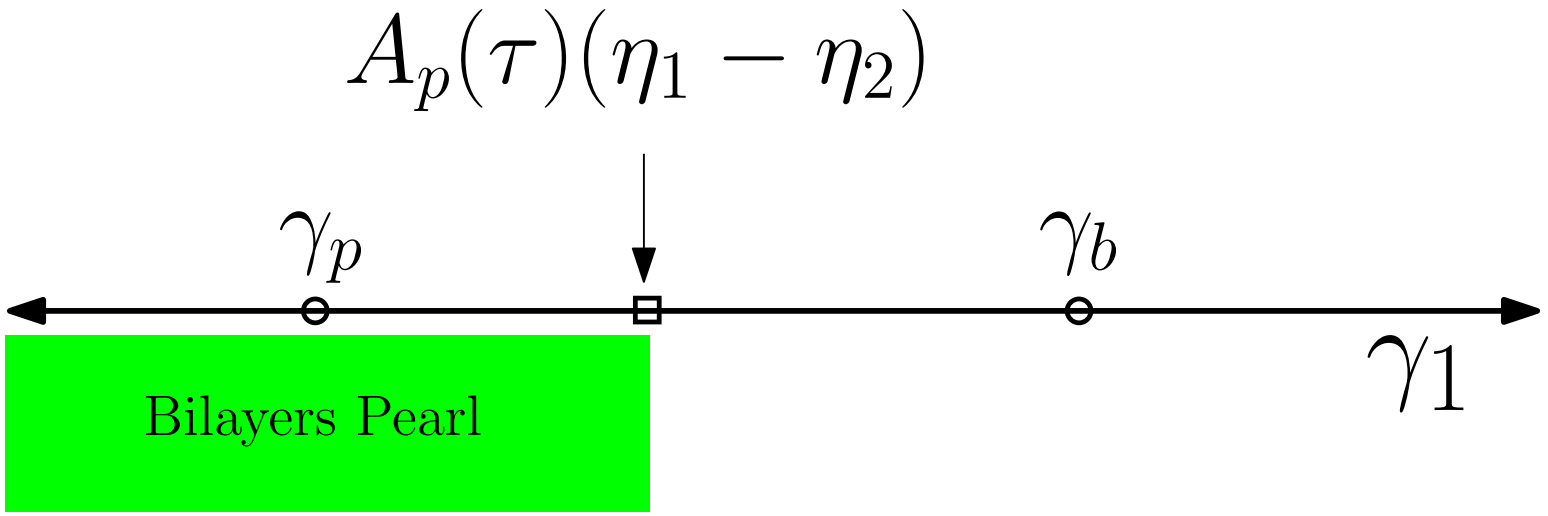

Coupled Geometric Evolution of Bilayers and Pores

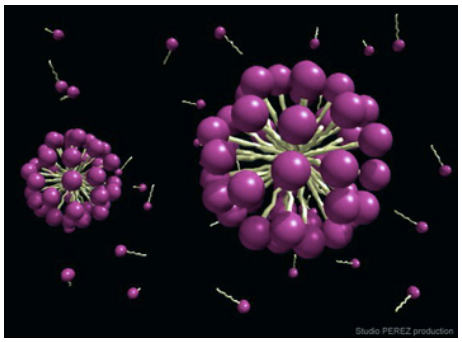

$$V_n = (\gamma_1 - \gamma_p(\tau))H$$
$$\vec{V}_p = (\gamma_1 - \gamma_p(\tau))\vec{\kappa}$$
$$\frac{d\gamma_1}{dt_1} = -(\gamma_1 - \gamma_p)\int_{\Gamma_b} H^2 dS + - \epsilon(\gamma_1 - \gamma_p)\int_{\Gamma_p} |\vec{\kappa}|^2 \, ds.$$

Relative size of $\gamma_p(\tau)$, $\gamma_b(\tau)$, and the pearling point $A_p(\tau)(\eta_1 - \eta_2)$ is crucial to dynamics.

$$A_p(\tau)(\eta_1 - \eta_2)$$

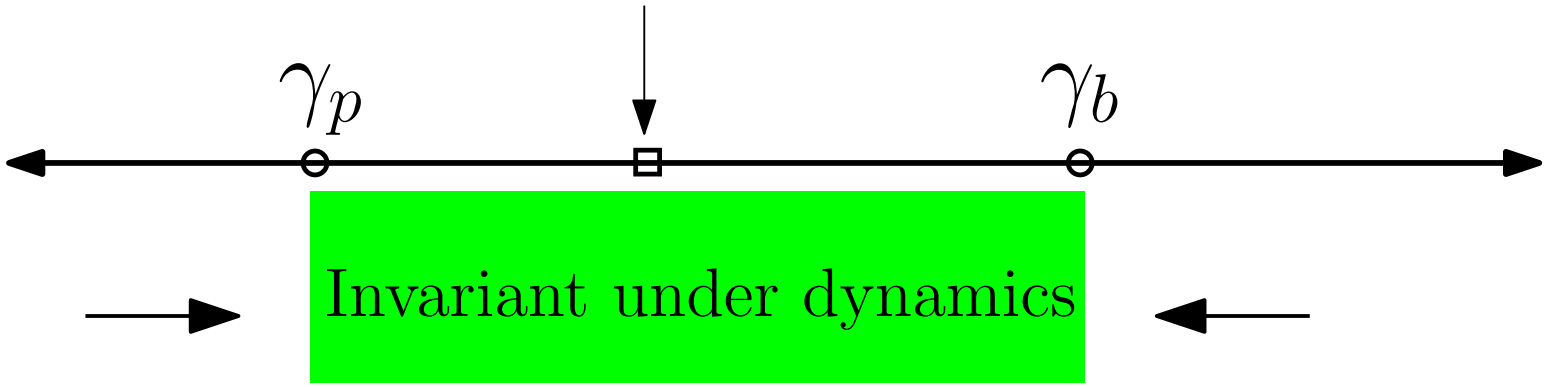

Competition and Pearling in Bilayers

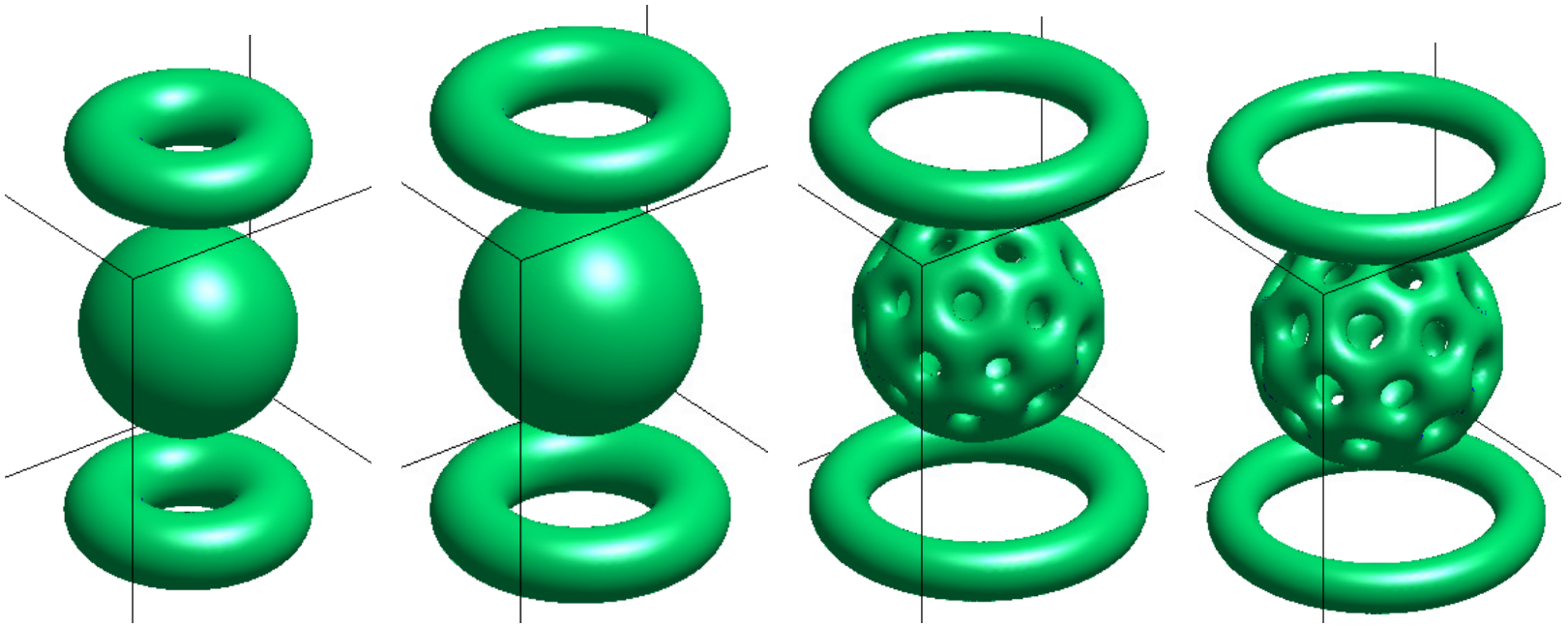

Competition for the amphiphilic phase between spherical bilayer (beach ball) and circular solid pore (hula hoop) as a function of the well-tilt. Well with small tilt prefers bilayers, larger tilt prefers pores and drives bilayers to pearl.

Punctured Vesicle - ETD

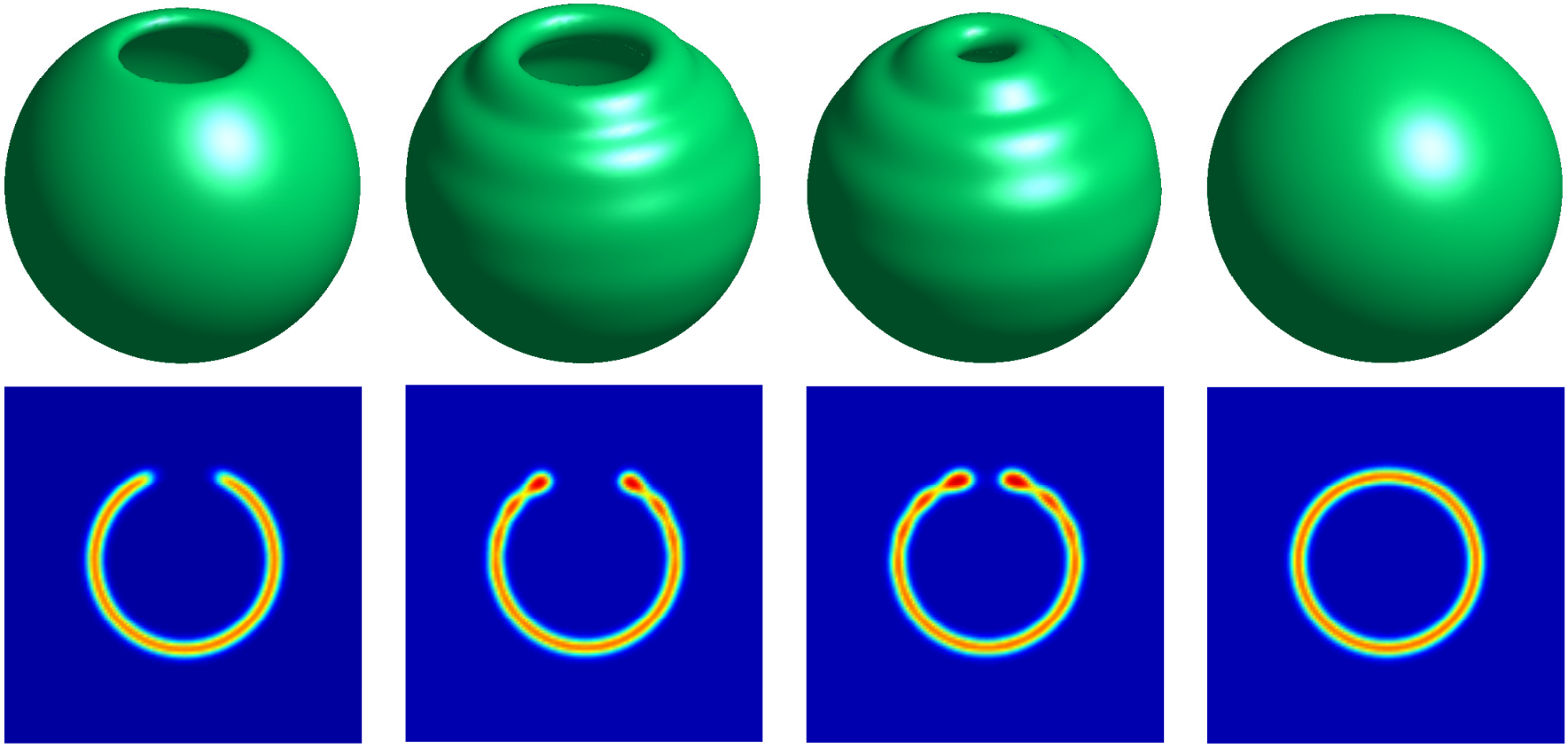

$T = 0$ $T = 0.5$ $T = 10.0$ $T = 15.0$

Time evolution of a punctured Bilayer under ETD. Under convex splitting vesicle failed to close.

Meander induces Endocytosis

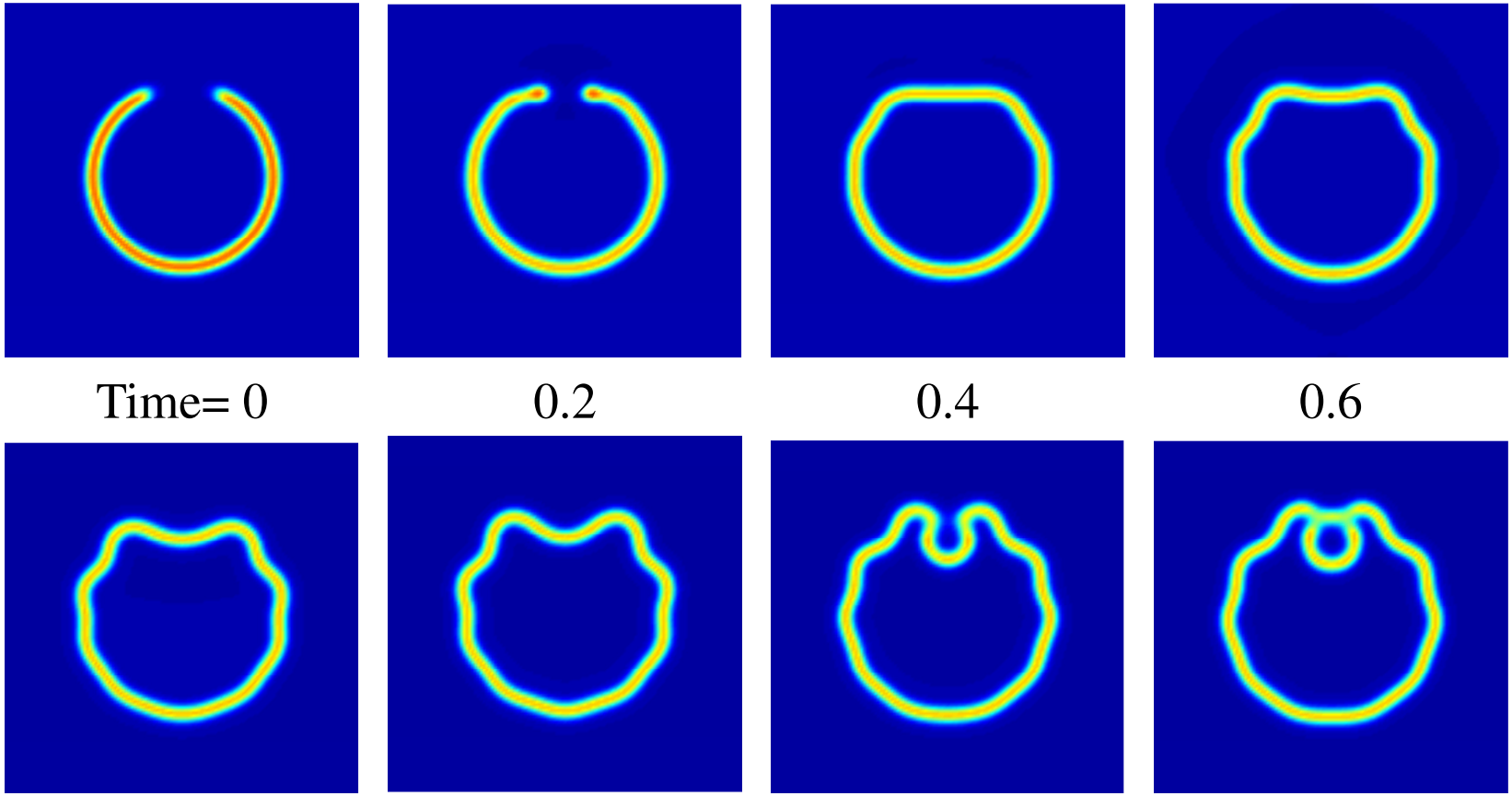

Cross sections of a punctured vesicle with too wide initial profile. Meandering induces endocytosis.

Intrinsic Curvature

The Canham-Helfrich sharp interface limit characterizes interfacial energy in terms of curvatures

$$E_{\mathrm{Can-Hel}}(\Gamma) = \int_{\Gamma} a_0(H - a_1)^2 + a_2 + a_3 K \, ds.$$

The term a_1 denotes the intrinsic curvature of the interface – and requires asymmetry.

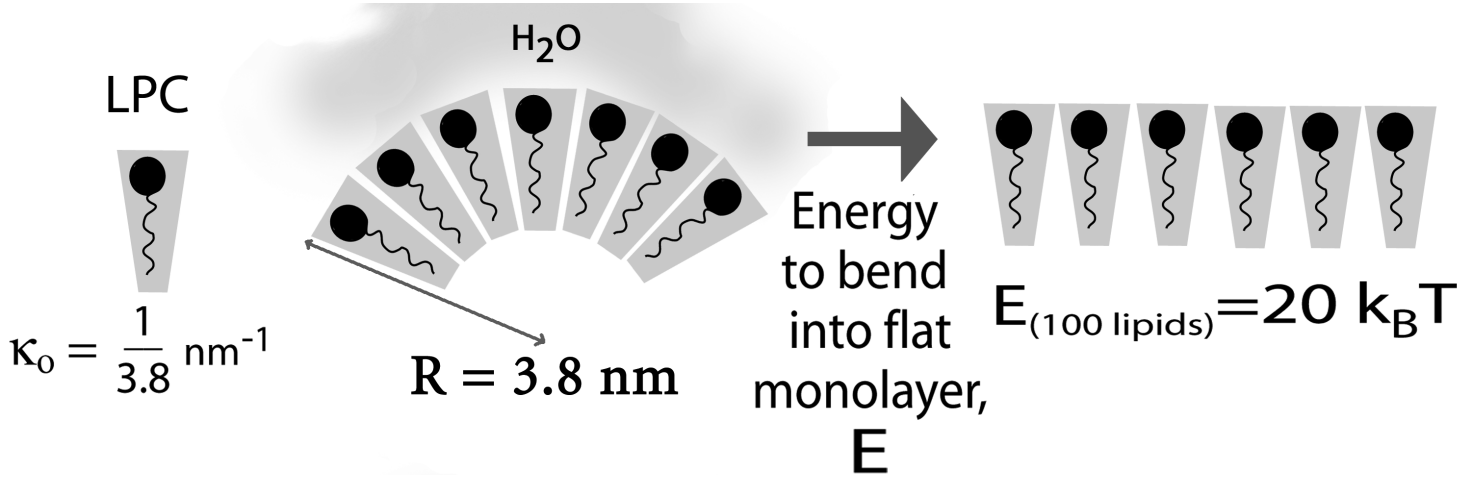

MCFCH: Pearling and Intrinsic Curvature in Bilayers

The multicomponent FCH in densities $\boldsymbol{U} = (\boldsymbol{U}_1, \ldots, \boldsymbol{U}_{N-1})$ takes form

$$\boldsymbol{\mathcal{F}}_{\mathrm{CH}}(\boldsymbol{U}) = \int_\Omega \frac{\mathbf{1}}{\mathbf{2}} \left|\boldsymbol{\epsilon}^2 \boldsymbol{D}\boldsymbol{\Delta}\boldsymbol{U} - \boldsymbol{\nabla}_{\boldsymbol{U}}\boldsymbol{W}(\boldsymbol{U})\right|^2 - \boldsymbol{\epsilon}^{\boldsymbol{p}} \left(\boldsymbol{\eta}_1 \frac{\boldsymbol{\epsilon}^2}{\mathbf{2}} |\boldsymbol{\nabla}\boldsymbol{U}|^2 + \boldsymbol{\eta}_2 \boldsymbol{W}(\boldsymbol{U})\right) \boldsymbol{dx},$$

where the well $\boldsymbol{W} : \mathbb{R}^{\boldsymbol{N-1}} \mapsto \mathbb{R}$.

Bilayers solve the leading order equation

$$\boldsymbol{U}_{zz} = \boldsymbol{D}^{-1}\boldsymbol{\nabla}_{\boldsymbol{U}}\boldsymbol{W}(\boldsymbol{U}),$$

which for a piece-wise smooth $\boldsymbol{W}$ can be understood in a frictionless billiard limit. It is easy to construct asymmetric bilayers in MC-FCH

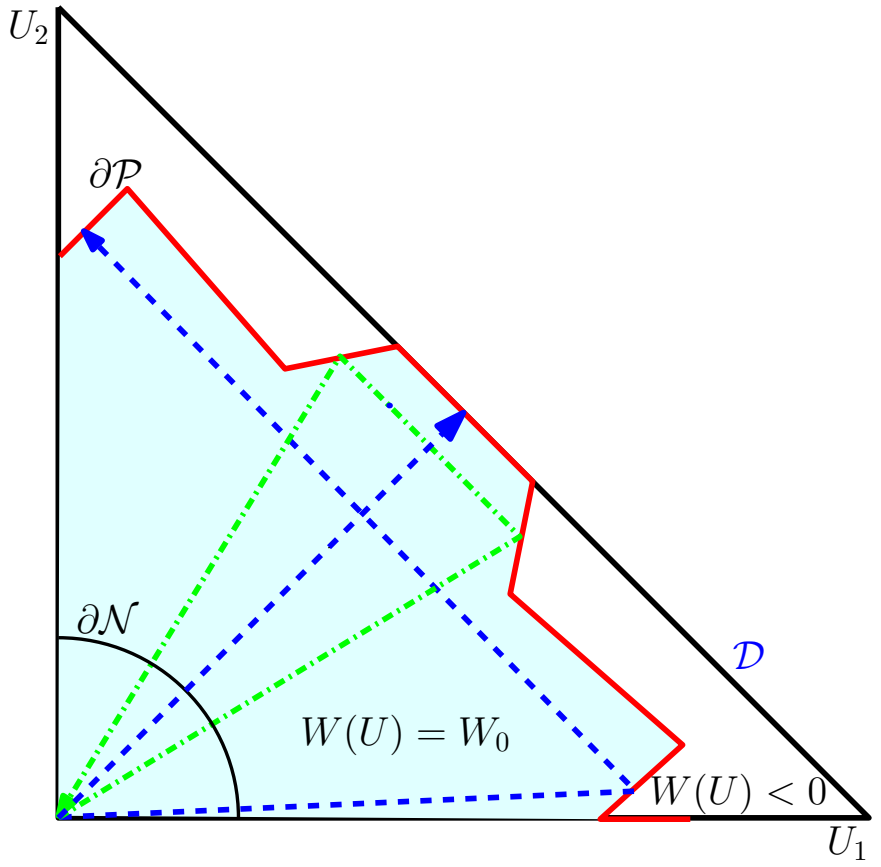

Pearling in amphiphilic di-block blends

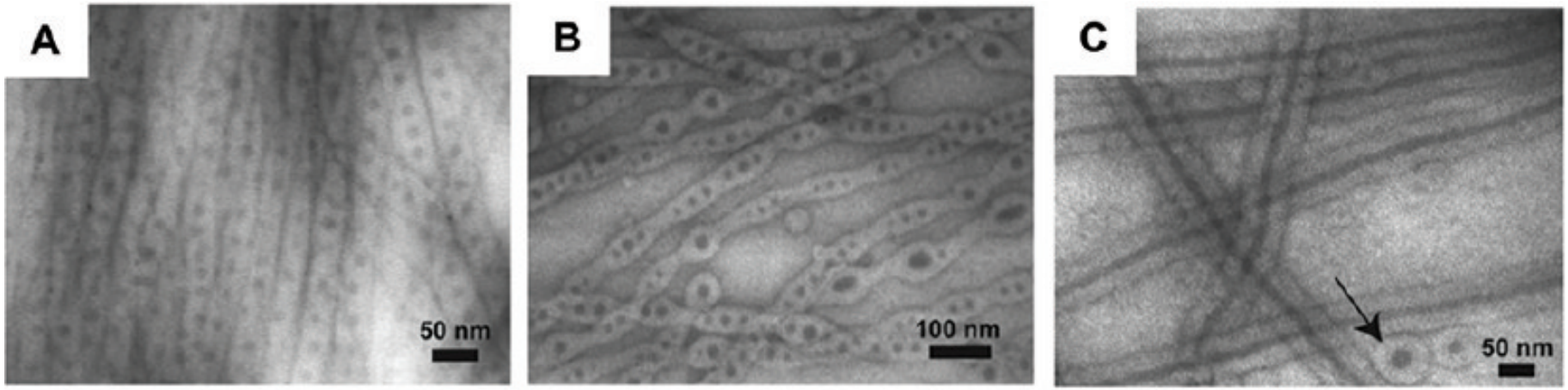

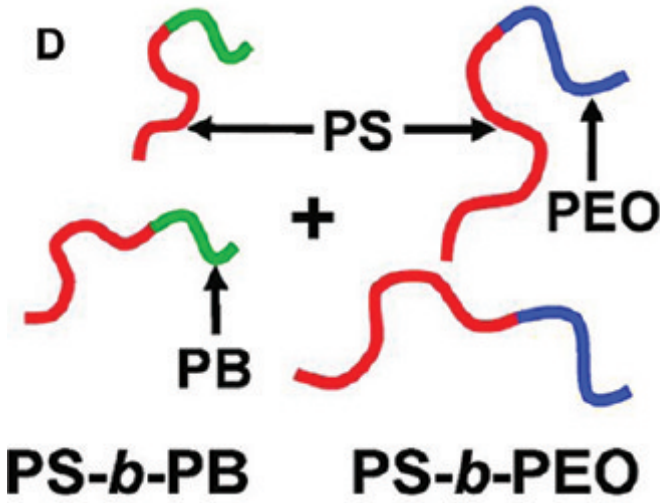

Changes in PS-PB and PS-PEO volume fractions (A) 80:20, (B) 70:30, (C) 60:40, drive pearling bifurcations in the internally separated phase. Hayward et al *Macro-molecules* (2008)

Instrinsic Curvature = Melnikov parameter

More generic MC-FCH has non-conservative term – $\nabla_U \times P(U) \neq 0$

$$\mathcal{F}_{\rm CH}(U) = \int_\Omega \frac{1}{2} \left|\epsilon^2 D\Delta U - \nabla_U W(U) - \epsilon P(U)\right|^2 - \epsilon^p G(U, \nabla U)\, dx,$$

The persistence of asymmetric bilayer solution requires a Melnikov parameter (a_1)

$$\boxed{V_{zz} + \epsilon a_1 V_z = D^{-1}\left(\nabla_U W(V) + \epsilon P(V)\right),}$$

where (asymmetry required!)

$$a_1 := \int_{\mathbb{R}} D^{-1} P(V) \cdot V_z\, dz \neq 0.$$

The co-dim one expansion of the square term takes the form

$$\epsilon^2 D\Delta U - \nabla_U W(U) + \epsilon P(U) = D(U_{zz} + \epsilon H(s) U_z) - \nabla_U W(U) - \epsilon P(U),$$

when evaluated at the homoclinic V has residual

$$|\epsilon^2 D\Delta V - \nabla_U W(V) + \epsilon P(V)|^2 = \epsilon^2 |DV_z|^2 |H(s) - a_1|^2 + O(\epsilon^3).$$

Integrate out the through-plane direction, remainder is a Canham-Helfrich energy

$$E(\Gamma) = \epsilon \int_\Gamma \left[\epsilon^2 \|DV_z\|_{L^2}^2 |H(s) - a_1|^2 - \epsilon^p \int_{\mathbb{R}} G(V, \nabla V) dz\right] ds$$

Acknowledgments

NSF-DMS 0934568 (Solar)
NSF-DMS 0929189 (IGMS)
NSF-DMS 1109127
NSF-DMS 1409940